

Selective Selenol Fluorescent Probes: Design, Synthesis, Structural Determinants, and Biological Applications

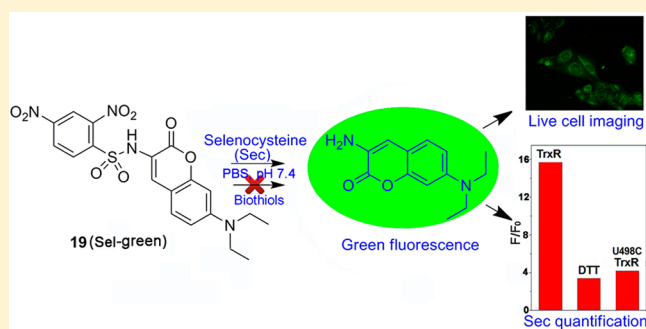
Baoxin Zhang, Chunpo Ge, Juan Yao, Yaping Liu, Huichen Xie, and Jianguo Fang*

State Key Laboratory of Applied Organic Chemistry and College of Chemistry and Chemical Engineering, Lanzhou University, Lanzhou, Gansu 730000, China

Supporting Information

ABSTRACT: Selenium (Se) is an essential micronutrient element, and the biological significance of Se is predominantly dependent on its incorporation as selenocysteine (Sec), the genetically encoded 21st amino acid in protein synthesis, into the active site of selenoproteins, which have broad functions, ranging from redox regulation and anti-inflammation to the production of active thyroid hormones. Compared to its counterpart Cys, there are only limited probes for selective recognition of Sec, and such selectivity is strictly restricted at low pH conditions. We reported herein the design, synthesis, and biological evaluations of a series of potential Sec probes based on the mechanism of nucleophilic aromatic substitution.

After the initial screening, the structural determinants for selective recognition of Sec were recapitulated. The follow-up studies identified that probe **19** (Sel-green) responds to Sec and other selenols with more than 100-fold increase of emission in neutral aqueous solution (pH 7.4), while there is no significant interference from the biological thiols, amines, or alcohols. Sel-green was successfully applied to quantify the Sec content in the selenoenzyme thioredoxin reductase and image endogenous Sec in live HepG2 cells. With the aid of Sel-green, we further demonstrated that the cytotoxicity of different selenocompounds is correlated to their ability metabolizing to selenols in cells. To the best of our knowledge, Sel-green is the first selenol probe that works under physiological conditions. The elucidation of the structure–activity relationship for selective recognition of selenols paves the way for further design of novel probes to better understand the pivotal role of Sec as well as selenoproteins in vivo.



INTRODUCTION

Selenium (Se) was recognized as an essential micronutrient element in 1960s.¹ Insufficient or excessive intake of Se has been associated with a number of diseases.^{2,3} Many different metabolites of Se, such as hydrogen selenide, selenocysteine (Sec), selenite, selenophosphate, selenodiglutathione, and charged Sec-tRNA, are synthesized in animals in the course of converting inorganic Se to organic forms and vice versa.^{2,4} Although Se may exist as different forms in vivo, the current knowledge of the biological significance of Se is predominantly dependent on its incorporation as the Sec into the active site of selenoproteins, which have a wide range of function, ranging from redox signaling and anti-inflammation to the production of active thyroid hormones.^{3,5,6} Sec is a cysteine (Cys) analogue with a selenium-containing selenol group in place of the sulfur-containing thiol group in Cys and the 21st amino acid in ribosome-mediated protein synthesis.^{7,8} Due to the low pK_a value of selenol (pK_a ~5.8),⁹ the Se in Sec is almost fully ionized under physiological conditions, which gives it high reactivity, and consequently Sec is normally essential for the catalytic efficiencies of selenoproteins.^{10,11} As the Sec carries out the majority function of the various Se-containing species in vivo, it is of high demand to develop reliable and rapid assays with biocompatibility to determine Sec.

Fluorescence sensing using small molecule probes has been one of the most powerful and popular tools to visualize the complicated biological processes. However, designing specific probes of Sec without suffering from the interference of biological thiols is a big challenge since the thiols usually present in high concentration (millimolar levels) in cells and have the similar chemical properties as Sec. The selenol pK_a value in Sec (~5.8) is lower than those of the most biological thiols (~8.3), which means that under physiological conditions (pH ~7.4) the Se in Sec is almost fully present as the selenolate (R-Se⁻), while the majority of thiols present as nonionized form (R-SH). The difference of pK_a values opens a window for selective detection of Sec in vitro by maintaining the reaction system under acidic condition. Maeda et al. reported the first fluorescent probe BESThio to discriminate the Sec from its counterpart Cys at pH 5.8.¹² We could also selectively label the Sec residue in the thioredoxin reductase (TrxR) by biotin-conjugated iodoacetamide at pH 6.5.^{13,14} However, all these assays are not compatible with the biological surroundings generally having a neutral environment (pH ~7.4), which prevents their practical applications in live system. Thus, it is of

Received: September 27, 2014

Published: January 5, 2015

Scheme 1. Sensing Thiols by the Mechanism of NAS

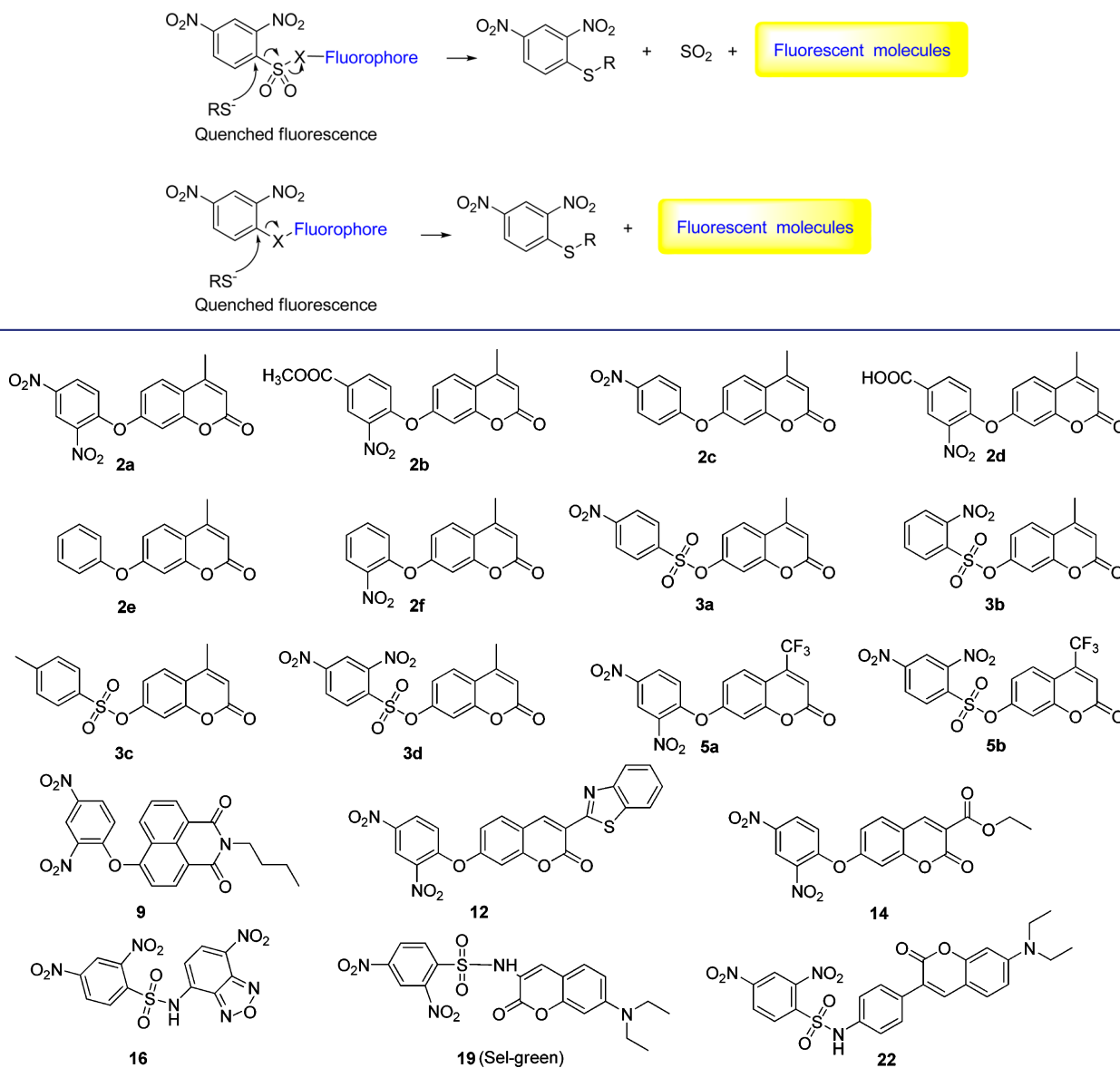


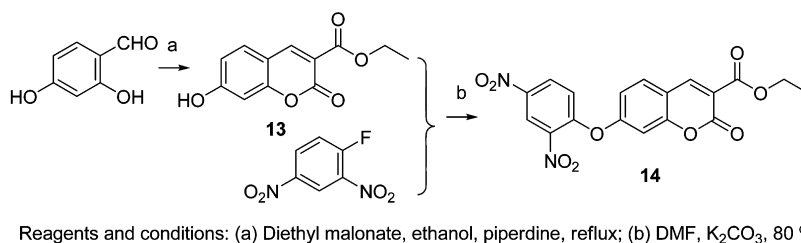
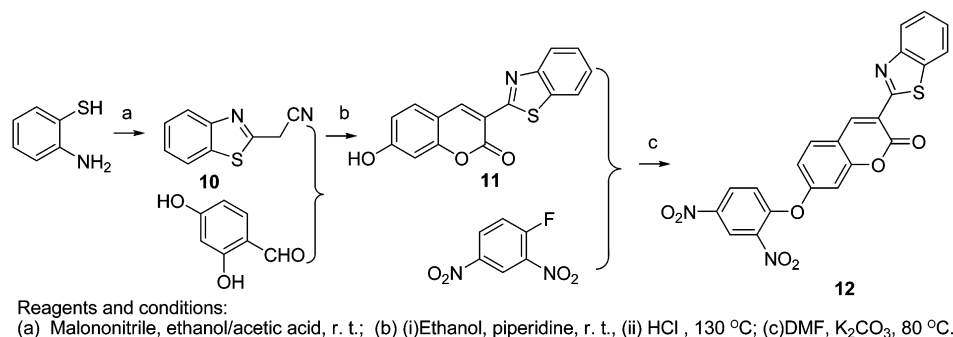
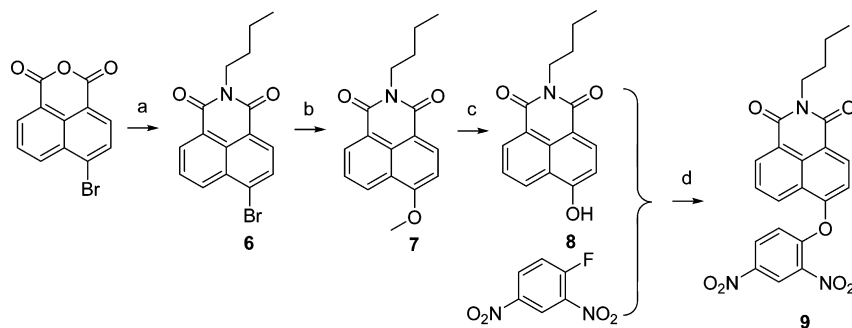
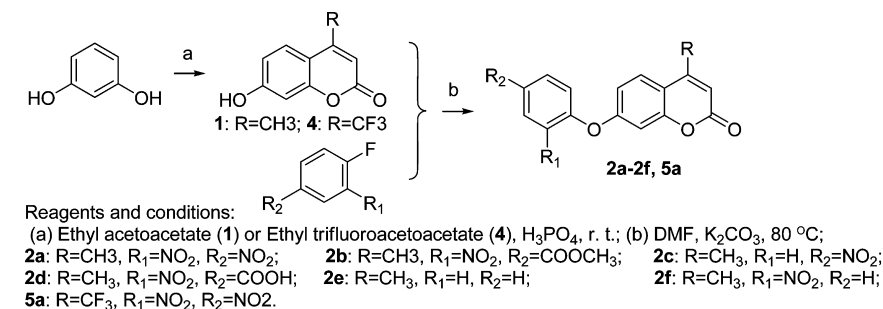
Figure 1. Chemical structures of probes.

great significance to develop novel probes that could selectively detect Sec over biological thiols under physiological conditions.

Based on the unique nucleophilicity of the sulfhydryl group, diverse thiol-selective probes have been rationally developed for activity-based protein profiling^{15–19} and thiol sensing.^{20–22} A well-elucidated mechanism for sensing thiols is the selective cleavage of 2,4-dinitrobenzyl functionality (a fluorescence quenching moiety) by thiols via nucleophilic aromatic substitution (NAS) (Scheme 1).^{23–25} This strategy utilizes the strong nucleophilicity of thiolates as well as the good leaving character of fluorophores. Inspired by this sensing mechanism and the better nucleophilicity of Sec (mainly present as selenolate) at neutral pH, we reasoned that we could adjust the electron density of the fluorescence quenching moiety and the linkage between the fluorophore and the quenching moiety. Via such modifications to tune the reactivity of the molecules, selective Sec probes at neutral pH might be discovered. As part of our continuing interest in discovering and developing novel small molecule regulators of cellular

redox systems,^{26–33} we reported herein the design, synthesis, and biological evaluations of a series of potential Sec probes (Figure 1). After an initial screening, the structural determinants for selective recognition of Sec were recapitulated. The follow-up studies disclosed that compound **19** (Sel-green) could respond to Sec and other selenols with more than 100-fold increase of emission in aqueous solution (pH 7.4), while there is no significant interference from the biological thiols, amines, or alcohols. Sel-green was successfully applied to quantify the Sec content in TrxR and image endogenous Sec in live HepG2 cells. In addition, Sel-green is suitable for identifying the selenol species metabolized from various selenocompounds in cells, which helps to clarify the mechanism underlying the cytotoxicity of different selenocompounds. To the best of our knowledge, Sel-green is the first selenol probe that works under physiological conditions. Furthermore, deciphering the structural determinants for selective selenol recognition paves the way for design and development of novel

Scheme 2. Synthesis of Ether Series Probes



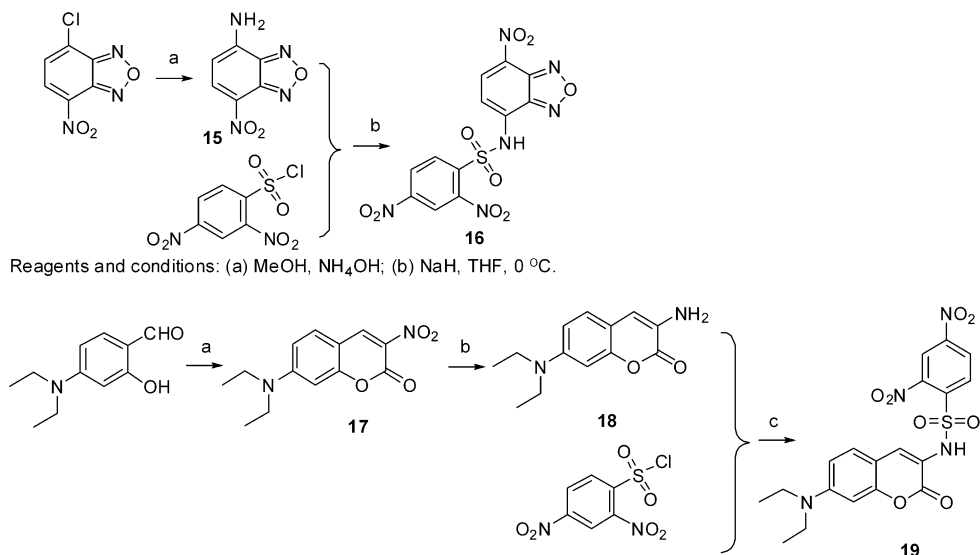
fluorescent probes with biocompatibility to understand the pivotal role of Sec and selenoproteins in vivo.

RESULTS AND DISCUSSION

Chemical Synthesis. The target probes were composed of three parts, i.e., fluorophores, electron-deficient quenching moieties and different linkages (Schemes 2, 3, and 4). The diverse fluorophores were constructed based on the coumarin and naphthalimide scaffolds due to their outstanding photophysical characters and easy preparation. The coupling of the fluorophores to the quenching moieties via ether, sulfonamide, or sulfonate linkage furnishes the final 18 probes (Figure 1). The straightforward synthetic routes were illustrated in Schemes 2–4. The original spectra (^1H NMR, ^{13}C NMR, and MS) of the final 18 compounds were included in the Supporting Information (Figures S3–S7).

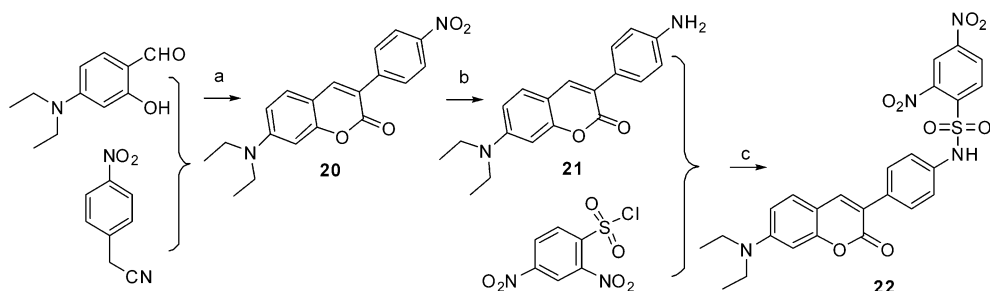
Structural Determinants for Selective Recognition of Sec. After we have constructed a series of potential probes, we screened their response to Sec and dithiothreitol (DTT) (Table 1). As Sec is not stable, we generated it in situ by mixing equal molar of DTT and selenocystine dimethyl ester ((Sec)₂).^{12,34} The probes were incubated with either DTT alone or Sec generated from DTT and (Sec)₂ for 5 min at room temperature in 0.1 M phosphate buffer solution (PBS), pH 7.4. The fluorescence intensity changes were measured and listed in Table 1. It is clear that the two nitro substitutions are essential, as removing or replacing them to other groups, such as methyl or carboxylic acid functionality, completely sacrifices the response to either DTT or Sec (compounds **2b–2f** and **3a–3c**). After introducing the 2,4-dinitrobenzene moiety, it appears that the character of linkages determines the probes' selectivity. Compounds with the sulfonate connection respond to both Sec

Scheme 3. Synthesis of Sulfonamide Series Probes

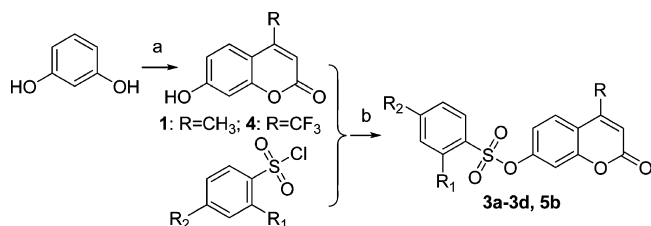


Reagents and conditions: (a) MeOH, NH_4OH ; (b) NaH, THF, 0°C .

Reagents and conditions: (a) $\text{NO}_2\text{CH}_2\text{COOC}_2\text{H}_5$, n-BuOH, reflux; (b) $\text{SnCl}_2\cdot 2\text{H}_2\text{O}$, r. t.; (c) DCM, TEA, r. t.



Reagents and conditions: (a) (i) Ethanol, piperidine, r. t., (ii) HCl (10%), 130°C ; (b) $\text{SnCl}_2\cdot 2\text{H}_2\text{O}$, r. t.; (c) DCM, TEA, r. t.

Scheme 4. Synthesis of Sulfonate Series Probes^a

^aReagents and conditions: (a) Ethyl acetoacetate (1) or ethyl trifluoroacetoacetate (4), H_3PO_4 , rt; (b) DCM, TEA, rt; 3a: $\text{R}=\text{CH}_3$, $\text{R}_1=\text{N}$, $\text{R}_2=\text{NO}_2$; 3b: $\text{R}=\text{CH}_3$, $\text{R}_1=\text{NO}_2$, $\text{R}_2=\text{H}$; 3c: $\text{R}=\text{CH}_3$, $\text{R}_1=\text{H}$, $\text{R}_2=\text{CH}_3$; 3d: $\text{R}=\text{CH}_3$, $\text{R}_1=\text{NO}_2$, $\text{R}_2=\text{NO}_2$; 5b: $\text{R}=\text{CF}_3$, $\text{R}_1=\text{NO}_2$, $\text{R}_2=\text{NO}_2$.

and DTT almost with the same potency, and thus could not discriminate the Sec from DTT (compounds 3d and 5b). This might attribute to the intrinsic higher reactivity of the sulfonate-bridged compounds. Molecules with ether or sulfonamide linkages exhibit promising selectivity (compounds 2a, 5a, 9, 12, 14, 16, 19, and 22). $(\text{Sec})_2$ alone gives no response. As several fluorophores display weak emission in aqueous solution (compounds 9, 12, and 22), a significant amount of organic solvents were included in assay buffer for these compounds.

Selective Recognition of Sec by 19. Further analysis of the data in Table 1 revealed that probes 9, 12, and 19 displayed

>20-fold selectivity of Sec over DTT. However, due to the intrinsic weak fluorescence of the fluorophores in 9 and 12 in aqueous solution, we picked up compound 19 for the follow-up studies. As 19 could be switched on to give green fluorescence, we termed it here as Sel-green. First, we determined the absorbance spectra of Sel-green upon addition of Sec. Sel-green has the maximum absorbance at around 400 nm in PBS buffer. After addition of Sec, its maximum absorbance is blue-shifted to ~ 370 nm (Figure 2A) with an isosbestic point at ~ 390 nm, indicating a clean reaction occurs. The response of Sel-green to Sec is fast, and the reaction completes within 3 min. The inset shows the time-dependent changes of absorbance at 401 and 371 nm. Determination of the fluorescence change is shown in Figure 2B. There is a marginal emission of Sel-green without Sec ($\phi < 0.001$). The emission intensity centered at 502 nm increased more than 100-fold after addition of Sec when excited at 370 nm ($\phi = 0.2$). The increment of fluorescence intensity is dependent on the incubation time, and the fluorescence intensity reaches a plateau after 3 min, consistent with the results from the absorbance spectra. The inset shows the time-dependent changes of emission at 502 nm. The fluorescence emission intensity at varying Sec concentrations (0–1 mM) was also determined and shown in Figure 2C, which clearly displays a manner of Sec concentration dependence. Figure 2D shows the dose-dependent changes of the emission at 502 nm. The response of Sel-green toward Sec is linear to the concentrations of the analyte with the range of 0–100 μM

Table 1. Response of Probes to Sec and DTT^a

probes	Sec ^b (F/F ₀)	DTT ^c (F/F ₀)	$\lambda_{\text{ex}}/\lambda_{\text{em}}$ (nm)	organic solvent ^d	selectivity (Sec/DTT)
2a	16.5	1.5	323/445	1% DMSO	11.0
2b	1.1	0.9	323/445	1% DMSO	1.2
2c	1.0	1.2	323/445	1% DMSO	0.8
2d	0.8	1.1	323/445	1% DMSO	0.7
2e	0.9	1.2	323/445	1% DMSO	0.8
2f	1.2	1.3	323/445	1% DMSO	0.9
3a	2.0	1.6	323/445	1% DMSO	1.2
3b	1.3	1.0	323/445	1% DMSO	1.3
3c	1.1	0.9	323/445	1% DMSO	1.2
3d	10.1	11.0	323/445	1% DMSO	0.9
5a	20.1	2.0	384/500	1% DMSO	10.0
5b	37.0	33.2	384/500	1% DMSO	1.1
9	25.0	1.2	467/553	40% DMSO	20.8
12	72.1	1.5	461/491	40% DMF	48.1
14	8.8	1.3	400/443	1% DMSO	6.8
16	25.8	2.3	465/550	— ^e	11.2
19 (Sel-green)	125	6.2	370/502	1% DMSO	20.2
22	2.96	1.1	410/500	40% DMSO	2.7

^aAssays were performed by incubating the probes (10 μM) with Sec or DTT for 5 min at room temperature. The fluorescence intensity changes were expressed as F/F_0 . ^bSec was generated in situ by mixing 50 μM of (Sec)₂ and 50 μM of DTT. ^cThe concentration of DTT is 50 μM . ^dThe probes, except 12 and 16, were dissolved in DMSO to create stock solutions, so in all assay buffers contain 1% of DMSO. Probe 12 was dissolved in DMF to create a stock solution. Due to the fluorophores of probes 9, 12, and 22 have very faint fluorescence in aqueous solution, 40% of DMSO, or DMF was introduced to facilitate the screening. ^eProbe 16 is soluble in water, and the stock solution of 16 was prepared in water. There is no organic solvent in the assay buffer.

($R = 0.9967$, inset in Figure 2D). The experimental detection limit is 0.5 μM , which displays a ~ 1.4 -fold increase of the fluorescence intensity with good reproducibility. The theoretical detection limit was calculated to be 62 nM with the equation of detection limit = $3\sigma/k$, where σ is the standard deviation of blank measurement, and k is the slope between the fold of fluorescence increase versus the Sec concentration.

The pH-dependent fluorescence change of Sel-green in recognition of Sec and Cys is shown in Figure 3A. The emission intensity increases as the pH rises and reaches a maximal value at ~ 7.4 . This attributes to that the higher pH facilitates the ionization of Sec to selenolate and hence promotes the NAS reaction to release the fluorophore. As the pH further increases from 7.4 to 9.0, the emission intensity decreases, which could be due to the instability of the lactone moiety in the fluorophore and the nonspecific reaction between Sec and Sel-green at higher pH. Sel-green exhibits stable response to Sec at the pH range of 6.0 to 7.7, indicating that it is suitable for applying under physiological environment. The response of Cys toward Sel-green has the similar trend as that of Sec, nevertheless with much less significance. The dynamic change of the fluorescence upon the reaction of Sel-green with Sec and Cys is shown in Figure 3B. Compared to the fast response of Sec, Cys gives a pretty sluggish reaction with Sel-green.

We then determined the selectivity of Sel-green toward the Sec. As shown in Figure 3C, amino acids without a sulfhydryl

group give no response to the probe. Vitamin C and inorganic sulfide are also negative to the probe. Cys, homocysteine (Hcy), and glutathione (GSH) at high concentration (1 mM for each) could trivially turn on the fluorescence. However, compared to the Sec (0.1 mM), this slight increase of fluorescence is negligible. The inset shows the photo of the Sel-green solution with Sec (0.1 mM, from 50 μM (Sec)₂ and 50 μM DTT), blank, and GSH (1 mM). As a control, DTT alone (50 μM) gives little response under the same conditions. The response of other selenocompounds, including Na₂SeO₃, Na₂Se, and benzenemethaneselenol (BzSeH, in situ generated from DBDS) was also measured, and only the BzSeH remarkably switches on the fluorescence. Collectively, Sel-green could selectively recognize selenols in neutral PBS buffer.

The reaction of Sel-green with Sec was further analyzed by HPLC. The retention times for Sel-green and the product 18 are 15.66 and 5.05 min, respectively (Figure S1A,B). After stirring the reaction containing Sel-green (48 mg, 0.1 mmol), (Sec)₂ (100 mg, 0.28 mmol) and DTT (42 mg, 0.28 mmol) in a DMSO-PBS mixed solvent (1:1, v/v) at room temperature for 1 h, the reaction mixture was extracted and the HPLC profiles were illustrated in Figure S1C,D. The remaining reactant (Sel-green) and the product (compound 18) were quantified to be 32.0 and 7.6 mg, respectively. The yield of formation of compound 18 is 33%. The conversion of Sel-green to the fluorophore 18 is 95%, indicating a clean conversion of Sel-green upon reacting with Sec.

Determination of Sec in TrxR. With these results in hands, we applied the probe Sel-green to analyze the Sec content in TrxR. The C-terminal extension with the motif -Gly-Cys-Sec-Gly carrying the essential Sec residue is unique for mammalian TrxRs. In the reduced TrxR, the Sec residue is exposed on the surface of the enzyme and easily accessible.^{35,36} Many small molecule inhibitors are known to interact with the enzyme by targeting the Sec residue at the active site.^{26,28–32,37,38} Thus, quantification of the content of the Sec residue is of great help to elucidate the mechanism of the interaction of small molecules with TrxR. The calibration curve of Sel-green was constructed, and a good linearity was obtained with the concentration of Sec ranging from 1 to 40 μM (Figure 3A). After addition of the recombinant rat TrxR (final concentration of 22 μM) and DTT (final concentration of 100 μM), the increase of fluorescence intensity was determined. According to the calibration curve, the Sec content in TrxR was calculated to be 16 μM . It should be noted that the recombinant TrxR used here contains both the full-length form and truncated form of the enzyme, which lacks the last two amino acids, i.e., Sec and Gly, at its C-terminus.^{39,40} The full-length enzyme is a homodimer and has one Sec residue in each subunit. The presence of the Sec-deficient truncated TrxR accounts for the lower Sec content (16 μM) from our result than the theoretical value (22 μM). We also determined the Sec content in the U498C TrxR, where the Sec498 was replaced by Cys. In stark contrast to the TrxR, the mutant enzyme only gives a background signal (Figure 3B), accentuating the specific recognition of Sec by Sel-green. Compared to DTT only, the slight higher fluorescence signal from the mutant enzyme with DTT could be due to the intrinsic fluorescence from the mutant enzyme, which contains a flavin molecule in each subunit. Many proteins bear reactive Cys residues with low pK_a values, such as Trx, Grx, PDI, and papain.^{41,42} The low pK_a Cys residues are generally created by the defined 3-D structure of proteins with some spatially neighboring acidic or basic

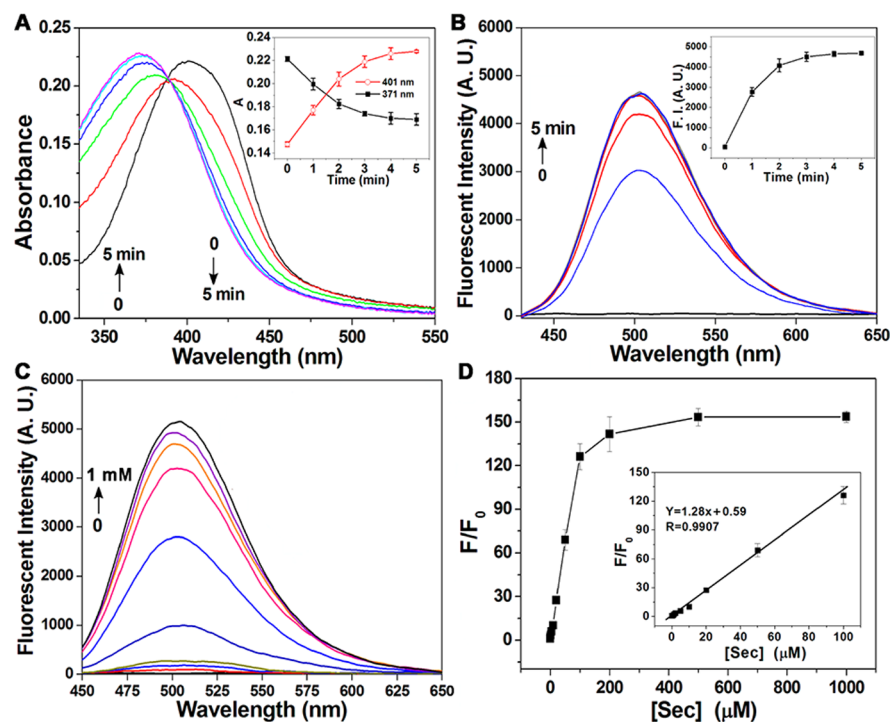


Figure 2. Response of Sel-green to Sec. (A). Time-dependent absorbance spectra of Sel-green toward Sec. Sel-green ($10 \mu\text{M}$) was incubated with DTT ($50 \mu\text{M}$) and $(\text{Sec})_2$ ($50 \mu\text{M}$) at room temperature in PBS, pH 7.4. The absorbance spectra were scanned every 1 min for 5 min. The arrows indicate the change of the spectra as the function of time. The inset shows the time-dependent changes of absorbance at 401 and 371 nm. (B). Time-dependent emission spectra of Sel-green toward Sec. Sel-green ($10 \mu\text{M}$) was incubated with DTT ($50 \mu\text{M}$) and $(\text{Sec})_2$ ($50 \mu\text{M}$) at room temperature in PBS, pH 7.4. The emission spectra ($\lambda_{\text{ex}} = 370 \text{ nm}$) were recorded every 1 min for 5 min. The arrow indicates the change of the spectra as the function of time. The inset shows the time-dependent changes of emission at 502 nm. (C). Dose-dependent emission spectra of Sel-green toward Sec. Sel-green ($10 \mu\text{M}$) was incubated with increasing concentrations of DTT and $(\text{Sec})_2$ at room temperature in PBS, pH 7.4. The emission spectra ($\lambda_{\text{ex}} = 370 \text{ nm}$) were recorded after 2 min. The arrow indicates the change of the spectra as the function of concentration. (D). Plotting the fold of fluorescence increase (F/F_0) at 502 nm ($\lambda_{\text{ex}} = 370 \text{ nm}$) versus the concentrations of Sec. The experimental conditions are the same as those in (C). The inset shows F/F_0 is linear to the concentrations of Sec in the range of 0.5–100 μM . Data were expressed as mean \pm standard deviation (SD) of three experiments.

residues. We further determined the response of Sel-green toward these proteins. As shown in Figure 4B, none of the tested proteins give significant response toward Sel-green. This observation is probably due to that Sel-green has little accessibility to the reactive Cys residues as they are usually buried within proteins to prevent their inactivation by electrophiles.

Exogenous and Endogenous Sec Imaging in Live Cells. The live cell imaging was performed in HepG2 cells. As the physiological concentration of Sec is low in cells, we first determine if Sel-green could respond to the exogenous Sec. After addition of $(\text{Sec})_2$ to the cultured HepG2 cells, a bright green fluorescence signal appears (Figure 5D,E), while there is no response in the control cells (Figure 5A,C). Another control experiment with the thiol probe BESThio indicates that the cellular thiols do not interfere with the detection of Sec by Sel-green (Figure 5B). This exciting observation motivates us to further determine the endogenous Sec in the cells. Sodium selenite (Na_2SeO_3) is a precursor of Sec biosynthesis, and supplement of cells with sodium selenite could significantly increase the Sec level in cells.⁴³ After the cells were stimulated with sodium selenite for 12 h, the notable fluorescence appeared (Figure 5G). A short time treatment (1h) gives weak but reproducible signal (Figure 5F). These results demonstrated that the probe Sel-green is suitable for imaging Sec in live cells.

Se is an essential element to humans. However, the overdose intake of Se or selenium-containing compounds is toxic. The toxicity of the selenocompounds is, at least in part, due to the metabolism of them to selenols, which react with cellular thiols to generate ROS via redox cycling.^{2,44} We then applied the probe to study the metabolism of different selenocompounds, including $(\text{Sec})_2$, SeO_2 , Na_2SeO_3 , Na_2SeO_4 , DBDS, BPS, and BPSO, in cells. Except Na_2SeO_4 , BPS and BPSO, all other selenocompounds significantly induce the green fluorescence in HepG2 cells at different time points (Figure 6), indicating the generation of selenol species. The similar results were also observed in HeLa cells (Figure S2). The fluorescence pictures were acquired under the same conditions. The slight high background in some pictures is probably due to the leakage of the fluorophore from the cells into the culture medium. Next, we determined the cytotoxicity of these selenocompounds to the HepG2 cells and HeLa cells. As shown in Figure 7, only the compounds which could be metabolized to selenol species cause significantly cytotoxicity. Thus, our results provide evidence to support that the cytotoxicity of selenocompounds is related to their ability to metabolize to selenol species.

One of the outstanding functions of Sec is that it is a key residue in several redox enzymes, such as glutathione peroxidase and TrxR.^{36,45} These redox enzymes regulate the diverse cellular redox signaling pathways, which are involved in cell proliferation, differentiation, and death. Together with thiols, Sec is increasingly recognized as an important

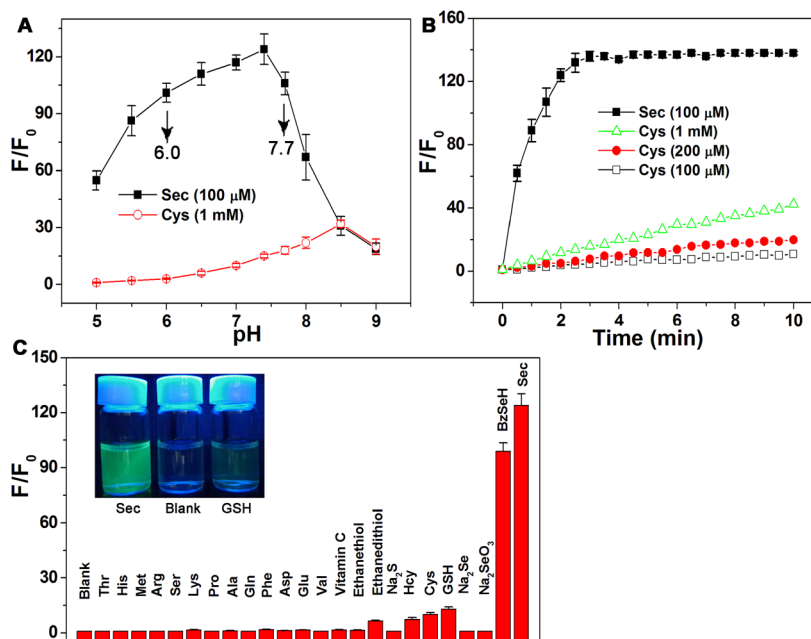


Figure 3. (A) Influence of pH on the response of Sel-green to Sec and Cys. The fold of fluorescence increase at 502 nm was determined after mixing Sel-green with Sec or Cys for 2 min in 0.1 M PBS buffers with the pH range from 5.0 to 9.0. Sec was generated from 50 μM DTT and 50 μM (Sec)₂. (B) Kinetics of the fluorescence change upon Sel-green responding to Sec and Cys. The fold of fluorescence increase at 502 nm was determined after mixing Sel-green with Sec or Cys at the indicated times in the PBS buffer, pH 7.4. The error bars for Cys were omitted for clarity, and the SD for each data point is less than 10%. (C) Selective recognition of Sec by Sel-green. The fold of fluorescence increase at 502 nm was determined after mixing Sel-green with various analytes for 2 min in the PBS buffer, pH 7.4. Sec was generated from 50 μM DTT and 50 μM (Sec)₂, and BzSeH was from 50 μM DTT and 50 μM DBDS. The concentration of other analytes is 1 mM. The photo of the inset was taken under UV illumination (365 nm). Data were expressed as mean ± SD of three experiments.

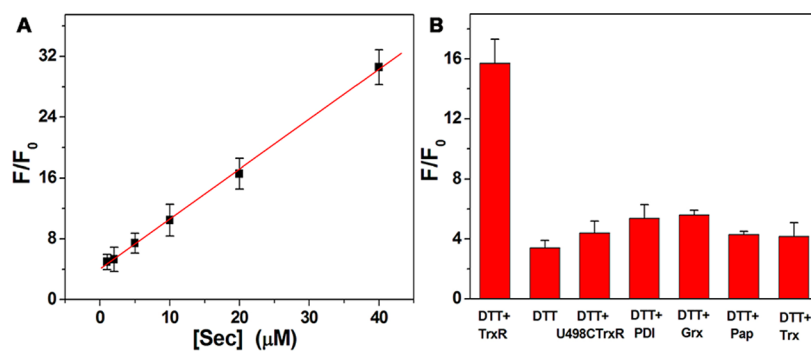


Figure 4. Response of Sel-green to selenoprotein TrxR and other proteins. (A). Calibration curve of response of Sel-green to Sec. (B). Response of Sel-green to TrxR, U498C TrxR, PDI, Grx, and Trx. The concentrations of the probe, DTT, and proteins are 50, 100, and 22 μM, respectively. The fluorescence intensity was read after incubation of the probe with the analytes at room temperature for 2 min. Data were expressed as mean ± SD of three experiments.

component of the cellular redox network.⁵ The literature is replete with the studies on the fluorescent probes of thiols, which were elegantly summarized in the recent reviews.^{20–22} However, the selective probes for Sec are quite limited, and the application of such probes was only restricted to the nonphysiological conditions.^{12–14} There is no Sec probe that can be used in neutral pH and live cells prior to this report. Based on the NAS sensing mechanism for thiols and the stronger nucleophilicity of selenols, we rationally synthesized a series of potential probes with varying reactivity. After careful evaluation, we discovered that Sel-green could selectively recognize selenols under physiological conditions. The potential disadvantage of Sel-green is its low sensitivity for cell imaging, which might limit its application *in vivo* due to the low amount of endogenous selenols. As illustrated in Figure 5,

the cellular fluorescence intensity is lower than that from the thiol probe BESThio (Figure 5B) but is significantly higher than that from the background (Figure 5C). Our SAR studies provide the structural determinants for selective recognition of selenols under physiological conditions, which will guide further development of novel probes with improved properties to understand the pivotal role of selenols as well as selenoproteins *in vivo*.

The mechanism of selective turn-on the fluorescence of Sel-green by Sec is illustrated in Scheme 5. The lower pK_a value of the selenol group renders Sec predominantly present as the selenolate form (R-Se⁻) at neutral pH. However, due to the higher pK_a value of thiols, the majority of the sulfhydryl group in a thiol is un-ionized and present as a neutral form (R-SH). The nucleophilic attack of the probe Sel-green by selenolate,

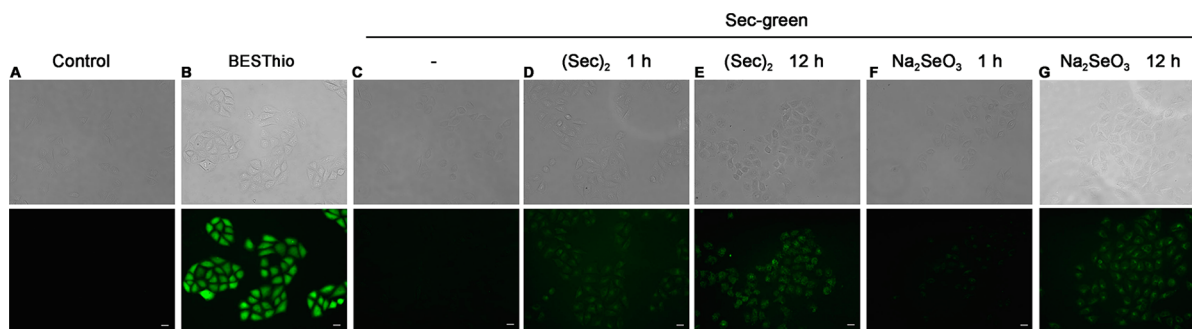


Figure 5. Imaging Sec in live HepG2 cells. The cells were treated with vehicle (A), the thiol probe BESThio ($20 \mu\text{M}$, B), and Sel-green ($20 \mu\text{M}$, C) for 30 min, and the bright-field images (top panel) and fluorescence images (bottom panel) were acquired. HepG2 cells were pretreated with $(\text{Sec})_2$ ($5 \mu\text{M}$) for 1 h (D) or 12 h (E) and Na_2SeO_3 ($5 \mu\text{M}$) for 1 h (F) or 12 h (G), followed by incubation with Sel-green ($20 \mu\text{M}$) for additional 30 min. The bright-field images (top panel) and fluorescence images (bottom panel) were acquired. The representative pictures were shown from three experiments. Scale bar: $15 \mu\text{m}$.

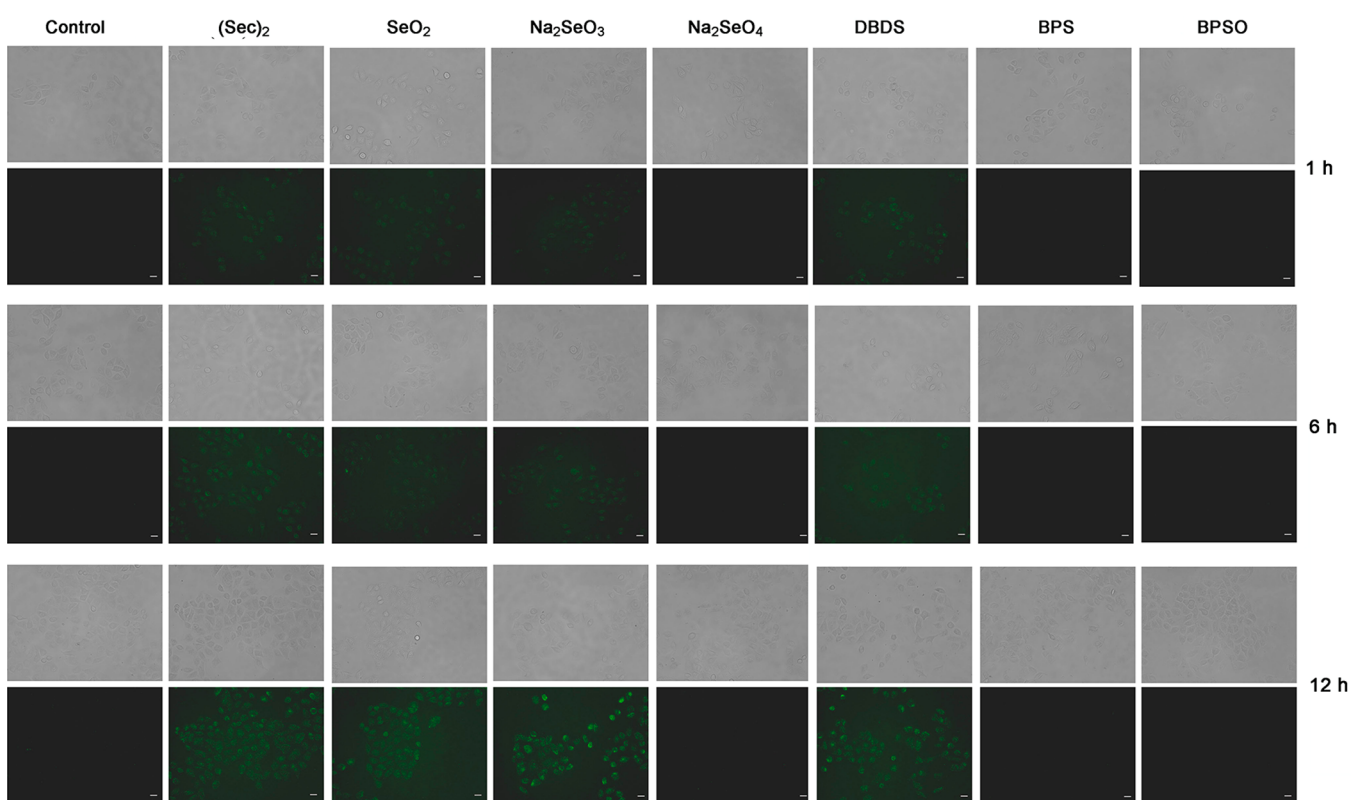


Figure 6. Imaging the metabolites of different selenocompounds in live HepG2 cells. The cells were pretreated with $5 \mu\text{M}$ of $(\text{Sec})_2$, SeO_2 , Na_2SeO_3 , Na_2SeO_4 , DBDS, BPS, and BPSO for 1, 6, or 12 h, followed by incubation with Sel-green ($20 \mu\text{M}$) for additional 30 min. The bright-field images (top panel) and fluorescence images (bottom panel) were acquired. The representative pictures were shown from three experiments. Scale bar: $15 \mu\text{m}$.

which is supposed to be a stronger nucleophile than thiols, would be favorable. Subsequently, the quenched fluorophore was released to trigger on the fluorescence. Several probes with sulfonamide linkage have been reported to selective recognize thiophenols at neutral pH.^{24,46–49} The thiophenols have pK_a values of ~ 6.5 , which are significantly lower than those of most aliphatic thiols. Thus, the selectivity of these probes toward thiophenols could follow the same mechanism as that of our probe Sel-green to Sec. However, compared to Sec, thiophenols are not naturally present in biological systems. We believe that the selective detection of Sec and other selenols is of high physiological significance.

CONCLUSIONS

In summary, we have rationally designed and prepared a series of potential selenol probes. After an initial screening, the structural determinants for selective recognition of selenol were delineated. The follow-up studies identified that Sel-green (**19**) could selectively respond to Sec and other selenols with more than 100-fold increase of emission in neutral aqueous solution (pH 7.4), while there is little interference from the biological thiols, amines, or alcohols. Sel-green was able to determine the selenol content in selenoprotein TrxR, while there is little response of the probe to the mutant enzyme U498C TrxR, demonstrating the specific recognition of Sec by the probe.

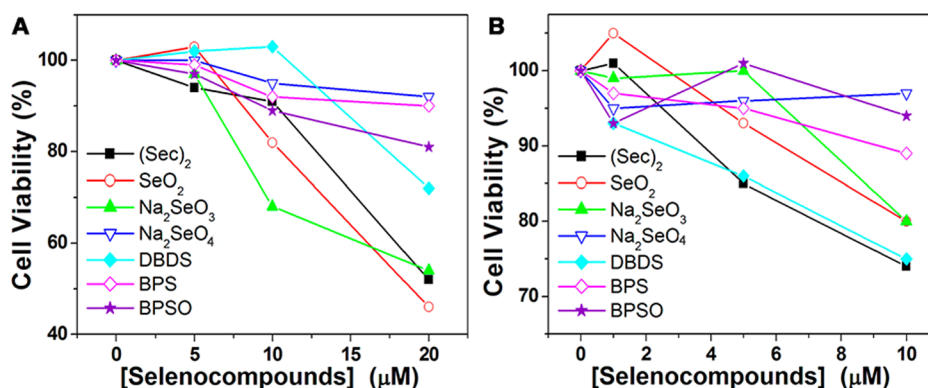
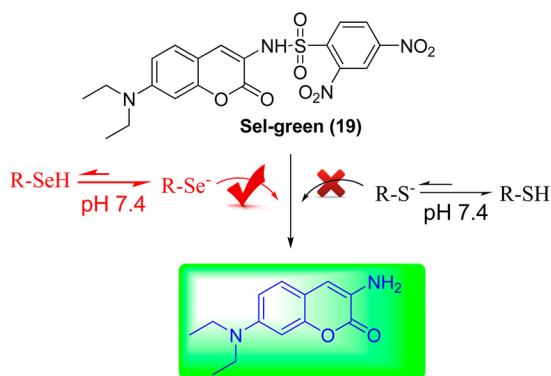


Figure 7. Cytotoxicity of selenocompounds. HepG2 (A) and HeLa (B) cells were treated with varying concentrations of different selenocompounds for 24 h, and the cell viability was determined by the MTT assay. Data were expressed the mean values from three experiments. The error bars were omitted for clarity, and the SD is <10% for each data point.

Scheme 5. Proposed Mechanism for Selective Recognition of Sec over Thiols



Finally, Sel-green was successfully applied to image the endogenous Sec in live HepG2 cells and disclose the involvement of selenol species for the cytotoxicity of selenocompounds. To the best of our knowledge, Sel-green is the first selective selenol probe that works under physiological conditions. Furthermore, deciphering the SAR of the selective selenol recognition paves the way for further development of novel fluorescent probes to understand the pivotal role of Sec as well as selenoproteins in vivo.

EXPERIMENTAL SECTION

Materials and Instruments. The recombinant rat TrxR was essentially prepared as described⁴⁰ and is a gift from Prof. Arne Holmgren at Karolinska Institute, Sweden. The recombinant U498C TrxR mutant (Sec → Cys) was produced as described.^{10,28} The HepG2 and HeLa cells were obtained from the Shanghai Institute of Biochemistry and Cell Biology, Chinese Academy of Sciences. Dulbecco's modified Eagle's medium (DMEM), GSH, dimethyl sulfoxide (DMSO), and dibenzyl diselenide (DBDS) were obtained from Sigma-Aldrich (St. Louis, MO, USA). Fetal bovine serum (FBS) was obtained from Sijiqing (Hangzhou, China). Papain and protein disulfide isomerase (PDI) were from Sangon Biotech (Shanghai, China). Thioredoxin (Trx) and glutaredoxin (Grx) from *E. coli* were from IMCO (Stockholm, Sweden, www.imcocorp.se). Penicillin and streptomycin were obtained from Sangon (Shanghai, China). Benzylphenylselenide (BPS) and benzylphenylselenoxide (BPSO) were synthesized according to the published refs 50 and 51. The thiol probe BESThio was synthesized according to the literature.^{12,25} All other reagents were of analytical grade and were purchased from commercial supplies. Absorption spectra were recorded on UV-vis spectrometer evolution 200 (Thermo Scientific). Fluorescence studies

were carried out using a LUMINA fluorescence spectrofluorometer (Thermo Scientific) at room temperature. MS spectra were recorded on Trace DSQ GC-MS spectrometer or Bruker Daltonics esquire 6000 mass spectrometer. HRMS was obtained on Orbitrap Elite (Thermo Scientific). The quantum yields (ϕ) of Sel-green with and without Sec were determined on FLS920 spectrometer (Edinburgh Instruments, U.K.) with $\lambda_{\text{ex}} = 370$ nm. ¹H and ¹³C NMR spectra were recorded on Bruker Advance 400, and tetramethylsilane (TMS) was used as a reference. (Sec)₂ was synthesized according to the literature⁵² in our laboratory.

Synthesis of Compound 1 (7-Hydroxy-4-methylcoumarin, Scheme 2).⁵³ 3-Hydroxyphenol (11 g, 100 mmol) and ethyl acetoacetate (13 mL, 100 mmol) were added to concentrated phosphoric acid (52 mL, 85%). After stirring at room temperature for 12 h, the reaction mixture was poured into 150 mL water. The crude product was collected by filtration and purified by recrystallization in ethanol to afford **1** as white crystal (19.3 g, yield 80%). ¹H NMR (400 MHz, DMSO-*d*₆) δ : 10.54 (s, 1H), 7.59 (d, *J* = 8.4 Hz, 1H), 6.81 (dd, *J* = 8.4, 2.0 Hz, 1H), 6.70 (d, *J* = 2.4 Hz, 1H), 6.12 (s, 1H), 2.35 (s, 3H); ¹³C NMR (100 MHz, DMSO-*d*₆) δ : 161.21, 160.34, 154.88, 153.31, 126.36, 112.84, 112.02, 110.31, 102.24, 18.08; mp: 189–190 °C. ESI-MS (*m/z*): [M + H]⁺ 177.1.

Synthesis of Compound 4 (7-Hydroxy-4-trifluoromethylcoumarin, Scheme 2).⁵³ 3-Hydroxyphenol (11 g, 100 mmol) and ethyl trifluoroacetoacetate (15 mL, 100 mmol) were added to concentrated phosphoric acid (52 mL, 85%). After stirring at room temperature for 12 h, the reaction mixture was poured into 150 mL water. The crude product was collected by filtration and purified by recrystallization in ethanol to afford **4** as white crystal (19.3 g, yield 80%). ¹H NMR (400 MHz, DMSO-*d*₆) δ : 10.96 (s, 1H), 7.55 (m, 1H), 6.91 (dd, *J* = 8.8, 2.4 Hz, 1H), 6.83 (t, 1H), 6.76 (d, *J* = 4.8 Hz, 1H); ¹³C NMR (100 MHz, DMSO-*d*₆) δ : 162.29, 158.82, 155.93, 140.33, 140.01, 139.70, 139.38, 126.00, 123.14, 120.40, 114.01, 105.15, 103.14; mp: 186–188 °C. ESI-MS (*m/z*): [M – H]⁺ 228.9.

Synthesis of Compounds 2a–2f and 5a. Compound **1** or **4** (0.6 mmol), substituted fluorobenzenes (1.0 mmol), and anhydrous potassium carbonate (414 mg, 3 mmol) were added to a three-necked flask under Ar atmosphere, and then anhydrous DMF (5 mL) was injected into the reaction flask with a syringe. The mixture was stirred at 80 °C until the starting material disappeared. The solvent was removed under reduced pressure, and the resulting residue was purified by chromatography on silica gel to give compound **2a–2f** and **5a**.

2a (7-(2,4-Dinitrophenoxy)-4-methylcoumarin, Scheme 2). ¹H NMR (400 MHz, DMSO-*d*₆) δ : 8.95 (d, *J* = 2.8 Hz, 1H), 8.52 (dd, *J* = 8.8, 2.4 Hz, 1H), 7.93 (d, *J* = 8.8 Hz, 1H), 7.43 (d, *J* = 9.2 Hz, 1H), 7.38 (d, *J* = 2.0 Hz, 1H), 7.29 (dd, *J* = 8.4, 2.0 Hz, 1H), 6.43 (s, 1H), 2.46 (s, 3H); ¹³C NMR (100 MHz, DMSO-*d*₆) δ : 159.93, 157.12, 154.73, 154.02, 153.38, 142.81, 140.43, 130.22, 128.14, 122.47, 121.51, 117.81, 116.30, 114.08, 108.16; mp: 186–187 °C; EI-MS (*m/z*) (%): 342(M⁺, 85), 175(79), 147(100).

2b (Methyl 4-(4-methyl-2-oxo-2H-chromen-7-yloxy)-3-nitrobenzoate, Scheme 2). ^1H NMR (400 MHz, DMSO- d_6) δ : 8.56 (s, 1H), 8.22 (d, J = 7.2 Hz, 1H), 7.88 (dd, J = 8.8, 4.0 Hz, 1H), 7.36 (dd, J = 8.4, 3.6 Hz, 1H), 7.27 (s, 1H), 7.20 (d, J = 8.0 Hz, 1H), 6.38 (s, 1H), 3.90 (s, 3H), 2.43 (s, 3H); ^{13}C NMR (100 MHz, DMSO- d_6) δ : 164.51, 159.98, 157.79, 154.73, 153.39, 152.63, 140.91, 135.99, 127.98, 127.39, 126.09, 121.74, 117.29, 115.83, 113.81, 197.51, 53.20, 18.62; mp: 164–165 °C; ESI-MS (m/z): $[\text{M} + \text{H}]^+$ 356.3.

2c (7-(4-Nitrophenoxy)-4-methylcoumarin, Scheme 2). ^1H NMR (400 MHz, CDCl_3) δ : 8.29 (d, J = 9.2 Hz, 2H), 7.66 (d, J = 8.0 Hz, 1H), 7.15 (d, J = 9.2 Hz, 2H), 7.04 (d, J = 8.4 Hz, 1H), 7.02 (d, J = 2.4 Hz, 1H), 6.28 (s, 1H), 2.46 (s, 3H); ^{13}C NMR (100 MHz, CDCl_3) δ : 161.86, 160.00, 157.79, 154.77, 153.37, 143.47, 127.89, 126.66, 119.01, 117.21, 116.48, 113.72, 108.13, 18.60; mp: 156–158 °C; ESI-MS (m/z): $[\text{M} + \text{H}]^+$ 298.3.

2d (4-(4-Methyl-2-oxo-2H-chromen-7-yloxy)-3-nitrobenzoic acid, Scheme 2). ^1H NMR (400 MHz, DMSO- d_6) δ : 13.56 (s, 1H), 8.55 (d, J = 1.6 Hz, 1H), 8.22 (dd, J = 8.8, 2.0 Hz, 1H), 7.87 (d, J = 8.8 Hz, 1H), 7.35 (d, J = 8.8 Hz, 1H), 7.26 (d, J = 2.4 Hz, 1H), 7.20 (dd, J = 8.8, 2.0 Hz, 1H), 6.38 (s, 1H), 2.44 (s, 3H); ^{13}C NMR (100 MHz, DMSO- d_6) δ : 165.57, 160.02, 158.07, 154.75, 153.41, 152.20, 140.97, 136.18, 127.94, 127.64, 127.46, 121.87, 117.15, 115.65, 113.73, 102.27, 18.63; mp: 230–232 °C; ESI-MS (m/z): $[\text{M} - \text{H}]^+$ 340.1.

2e (7-Phenoxy-4-methylcoumarin, Scheme 2). ^1H NMR (400 MHz, CDCl_3) δ : 7.56 (d, J = 8.8 Hz, 1H), 7.44 (t, 2H), 7.25 (t, 1H), 7.10 (d, J = 8.0 Hz, 2H), 6.97 (dd, J = 8.8, 2.4 Hz, 1H), 6.87 (d, J = 2.4 Hz, 1H), 6.19 (s, 1H), 2.42 (s, 3H); ^{13}C NMR (100 MHz, CDCl_3) δ : 160.56, 160.20, 155.38, 154.80, 153.53, 130.78, 127.52, 125.29, 120.28, 115.47, 114.46, 112.74, 105.33, 18.56; mp: 59–60 °C; ESI-MS (m/z): $[\text{M} + \text{H}]^+$ 253.2.

2f (7-(2-Nitrophenoxy)-4-methylcoumarin, Scheme 2). ^1H NMR (400 MHz, CDCl_3) δ : 8.16 (t, 1H), 7.80 (m, 2H), 7.52 (t, 1H), 7.39 (d, J = 8.0 Hz, 1H), 7.04 (t, 2H), 6.33 (s, 1H), 2.41 (s, 3H); ^{13}C NMR (100 MHz, CDCl_3) δ : 160.09, 159.53, 154.74, 153.46, 147.89, 142.01, 135.97, 127.71, 126.45, 123.28, 116.22, 114.29, 113.21, 105.56, 102.57, 18.59; mp: 132–134 °C; ESI-MS (m/z): $[\text{M} + \text{H}]^+$ 298.3.

5a (7-(2,4-Dinitrophenoxy)-4-trifluoromethylcoumarin, Scheme 2). ^1H NMR (400 MHz, DMSO- d_6) δ : 8.96 (d, J = 2.8 Hz, 1H), 8.63 (dd, J = 9.2, 2.8 Hz, 1H), 7.92 (dd, J = 8.8, 1.6 Hz, 1H), 7.66 (d, J = 9.2 Hz, 1H), 7.38 (d, J = 2.8 Hz, 1H), 7.36 (d, J = 2.0 Hz, 1H), 6.94 (s, 1H); ^{13}C NMR (100 MHz, DMSO- d_6) δ : 158.58, 158.25, 155.82, 153.28, 143.36, 140.83, 130.37, 127.38, 122.54, 122.43, 116.90, 116.80, 110.98, 108.54; mp: 162–163 °C, EI-MS (m/z) (%): 396(M^+ , 40), 229(33), 167(100).

Synthesis of Compounds 3a–3d and 5b. The substituted benzenesulfonyl chloride (1.0 mmol) in 5 mL of CH_2Cl_2 was slowly added to the solution of compound 1 or 4 (1.2 mmol) and Et_3N (200 mg, 2 mmol) in 20 mL of CH_2Cl_2 . The mixture was stirred overnight at room temperature. After the reaction was completed, the mixture was extracted with CH_2Cl_2 and dried with anhydrous Na_2SO_4 . After removing the solvent under reduced pressure, the residue was purified by flash column chromatography to give compound 3a–3d and 5b.

3a (4-Methyl-2-oxo-2H-chromen-7-yl-4-nitrobenzenesulfonate, Scheme 4). ^1H NMR (400 MHz, DMSO- d_6) δ : 8.48 (m, 2H), 8.22 (m, 2H), 7.82 (d, J = 8.8 Hz, 1H), 7.26 (d, J = 2.4 Hz, 1H), 7.14 (dd, J = 8.8, 2.4 Hz, 1H), 6.45 (d, J = 1.2 Hz, 1H), 2.41 (s, 3H); ^{13}C NMR (100 MHz, DMSO- d_6) δ : 159.59, 153.83, 152.96, 151.61, 150.69, 139.45, 130.55, 127.67, 125.56, 119.60, 118.60, 115.15, 110.92, 18.54; mp: 184–185 °C; ESI-MS (m/z): $[\text{M} + \text{H}]^+$ 362.3.

3b (4-Methyl-2-oxo-2H-chromen-7-yl-2-nitrobenzenesulfonate, Scheme 4). ^1H NMR (400 MHz, DMSO- d_6) δ : 8.24 (d, J = 8.0 Hz, 1H), 8.11 (d, J = 7.2 Hz, 1H), 8.06 (d, J = 8.0 Hz, 1H), 7.92 (t, 1H), 7.83 (d, J = 8.8 Hz, 1H), 7.26 (s, 1H), 7.17 (d, J = 8.0 Hz, 1H), 6.43 (s, 1H), 2.39 (s, 3H); ^{13}C NMR (100 MHz, DMSO- d_6) δ : 159.54, 153.85, 152.92, 150.57, 148.34, 137.76, 133.70, 132.30, 127.76, 126.23, 126.06, 119.72, 118.40, 115.22, 110.78, 18.53; mp: 181–182 °C; ESI-MS (m/z): $[\text{M} + \text{H}]^+$ 362.2.

3c (4-Methyl-2-oxo-2H-chromen-7-yl-4-methylbenzenesulfonate, Scheme 4). ^1H NMR (400 MHz, DMSO- d_6) δ : 7.80 (t, 3H), 7.50 (d, J = 8.0 Hz, 2H), 7.13 (d, J = 2.4 Hz, 1H), 7.07 (dd, J = 8.8, 2.4

Hz, 1H), 6.42 (d, J = 1.6 Hz, 1H), 2.42 (s, 3H), 2.40 (s, 3H); ^{13}C NMR (100 MHz, DMSO- d_6) δ : 159.61, 153.73, 152.97, 151.14, 146.60, 135.68, 133.59, 131.41, 130.77, 128.72, 127.42, 119.17, 118.52, 114.91, 110.70, 21.59, 18.51; mp: 92–95 °C; ESI-MS (m/z): $[\text{M} + \text{H}]^+$ 331.2.

3d (4-Methyl-2-oxo-2H-chromen-7-yl-2,4-dinitrobenzenesulfonate, Scheme 4). ^1H NMR (400 MHz, DMSO- d_6) δ : 9.12 (s, 1H), 8.63 (d, J = 8.0 Hz, 1H), 8.32 (d, J = 8.4 Hz, 1H), 7.85 (d, J = 8.4 Hz, 1H), 7.32 (s, 1H), 7.23 (d, J = 8.0 Hz, 1H), 6.44 (s, 1H), 2.41 (s, 3H); ^{13}C NMR (100 MHz, DMSO- d_6) δ : 159.52, 153.92, 152.90, 152.02, 150.37, 148.57, 134.10, 131.01, 128.09, 127.86, 121.69, 119.95, 118.54, 115.35, 110.85, 18.57; mp: 187–188 °C; ESI-MS (m/z): $[\text{M} + \text{H}]^+$ 407.2.

5b (4-Trifluoromethyl-2-oxo-2H-chromen-7-yl-2,4-dinitrobenzenesulfonate, Scheme 4). ^1H NMR (400 MHz, DMSO- d_6) δ : 9.12 (s, 1H), 8.64 (t, 1H), 8.35 (d, J = 8.8 Hz, 1H), 7.80 (d, J = 8.4 Hz, 1H), 7.54 (s, 1H), 7.32 (t, 1H), 7.16 (s, 1H); ^{13}C NMR (100 MHz, DMSO- d_6) δ : 158.21, 154.99, 152.09, 150.91, 148.54, 134.05, 130.97, 128.18, 127.21, 121.76, 120.50, 119.42, 118.83, 118.77, 113.62, 111.96; mp: 125–126 °C; ESI-MS (m/z): $[\text{M} + \text{H}]^+$ 461.2.

Synthesis of Compound 8 (4-Hydroxy-*n*-butyl-1,8-naphthalimide, Scheme 2). A mixture of 7 (2.08 g, 7.3 mmol), which was prepared according to the literature from 4-bromo-1,8-naphthalic anhydride via two steps,⁵⁴ and 57% (v/v) hydroiodic acid (100 mL) was refluxed under argon for 10 h. After cooling, the resulting mixture was filtered, then the crude product was washed with water to afford yellow-green solid. The crude product was purified by column chromatography on silica gel to afford compound 8 as a pale yellow solid (0.88 g, yield 45%). ^1H NMR (400 MHz, DMSO- d_6) δ : 11.83 (s, 1H), 8.54 (dd, J = 8.4, 1.2 Hz, 1H), 8.48 (dd, J = 7.2, 1.2 Hz, 1H), 8.36 (d, J = 8.4 Hz, 1H), 7.78 (d, J = 7.6 Hz, 1H), 7.16 (d, J = 8.4 Hz, 1H), 4.03 (t, 2H), 1.63 (m, 2H), 1.38 (m, 2H), 0.93 (t, 3H); ^{13}C NMR (100 MHz, DMSO- d_6) δ : 163.64, 162.96, 160.20, 133.51, 131.09, 129.16, 128.85, 125.59, 122.36, 121.81, 112.61, 109.94, 29.72, 19.77, 13.68; mp: 165–166 °C. ESI-MS (m/z): $[\text{M} - \text{H}]^+$ 268.5.

Synthesis of Compound 9 (4-(2,4-Dinitrophenoxy)-*n*-butyl-1,8-naphthalimide, Scheme 2).⁵⁵ 2,4-Dinitrofluorobenzene (186 mg, 1.0 mmol), compound 8 (134 mg, 0.5 mmol), and anhydrous potassium carbonate (414 mg, 3 mmol) were added to a three-necked flask under Ar atmosphere, and anhydrous DMF (5 mL) was injected into the reaction flask with a syringe. The mixture was stirred at 80 °C until the starting material disappeared. The solvent was removed under reduced pressure, and the resulting residue was purified by chromatography on silica gel to give compound 9 (217 mg, yield 50%). ^1H NMR (400 MHz, CDCl_3) δ : 8.99 (d, J = 2.8 Hz, 1H), 8.71 (dd, J = 7.6, 1.2 Hz, 1H), 8.60 (d, J = 8.0 Hz, 1H), 8.49 (d, J = 1.2 Hz, 1H), 8.47 (dd, J = 9.2, 2.8 Hz, 1H), 7.87 (m, 1H), 7.25 (dd, J = 8.0, 1.2 Hz, 2H), 4.21 (t, 2H), 1.76 (m, 2H), 1.50 (m, 2H), 1.00 (t, 3H); ^{13}C NMR (100 MHz, CDCl_3) δ : 163.66, 163.05, 155.21, 153.90, 143.11, 140.52, 132.34, 131.82, 129.71, 129.26, 127.86, 127.54, 124.06, 122.99, 122.38, 121.05, 120.19, 114.40, 40.30, 30.10, 20.30, 13.79; mp: 179–180 °C. EI-MS (m/z) (%): 435(M^+ , 3), 268(100), 44(40).

Synthesis of Compound 11 (7-Hydroxy-3-benzo[d]thiazol-2-ylcoumarin, Scheme 2). 2,4-Dihydroxybenzaldehyde (345.3 mg, 2.5 mmol) and compound 10 (435.55 mg, 2.55 mmol), which was prepared according to the literature^{23,56} from 2-aminobenzenethiol, were dissolved in 5 mL ethanol, and five drops of piperidine were added. The mixture was stirred at room temperature overnight. After filtration, the yellow solid was treated with 10% hydrochloric acid. The suspended solution was stirred at 130 °C overnight, and the resulting yellow residue was collected by filtration, washed with water, dried under reduced vacuum, and then purified by silica gel column chromatography to afford compound 11 (515 mg, yield 70%). ^1H NMR (400 MHz, DMSO- d_6) δ : 11.13 (s, 1H), 9.13 (s, 1H), 8.14 (d, J = 7.6 Hz, 1H), 8.03 (d, J = 8.0 Hz, 1H), 7.90 (d, J = 8.4 Hz, 1H), 7.55 (m, 1H), 7.45 (t, 1H), 6.93 (dd, J = 8.8, 2.4 Hz, 1H), 6.86 (d, J = 2.0 Hz, 1H); ^{13}C NMR (100 MHz, DMSO- d_6) δ : 163.45, 160.38, 159.75, 155.73, 151.95, 142.63, 135.59, 131.90, 126.45, 124.95, 122.14, 122.06, 114.51, 114.43, 111.40, 102.01; mp: >300 °C. ESI-MS (m/z): $[\text{M} + \text{H}]^+$ 296.0.

Synthesis of Compound 12 (7-(2,4-Dinitrophenoxy)-3-benzo[d]thiazol-2-ylcoumarin, Scheme 2).²³ Compound 11 (59 mg, 0.2 mmol), 2,4-dinitrofluorobenzene (111.6 mg, 0.6 mmol), and anhydrous potassium carbonate (276 mg, 2 mmol) were added to a three-necked flask under Ar atmosphere, and anhydrous DMF (3 mL) was injected into the reaction flask with a syringe. The mixture was stirred at 80 °C for 8 h. The solvent was removed under reduced pressure, and the resulting residue was purified by chromatography on silica gel to give compound 12 (64.5 mg, yield 70%). ¹H NMR (400 MHz, DMSO-*d*₆) δ: 9.31 (s, 1H), 8.97 (d, *J* = 2.8 Hz, 1H), 8.57 (dd, *J* = 9.2, 2.8 Hz, 1H), 8.24 (t, 2H), 8.11 (d, *J* = 8.0 Hz, 1H), 7.62 (t, 1H), 7.54 (m, 3H), 7.39 (dd, *J* = 8.4, 2.4 Hz, 1H); ¹³C NMR (100 MHz, DMSO-*d*₆) δ: 160.12, 159.64, 158.88, 155.28, 153.46, 152.39, 143.35, 141.96, 140.84, 136.37, 132.91, 130.40, 127.19, 125.93, 122.97, 122.72, 122.57, 122.44, 118.94, 117.05, 116.84, 107.45; mp: 248–250 °C. ESI-MS (*m/z*): [M + H]⁺ 462.3.

Synthesis of Compound 13 (Ethyl-7-hydroxy-2-oxo-2H-chromene-3-carboxylate, Scheme 2).⁵⁷ Diethyl malonate (6.96 g, 43.45 mmol), 2,4-dihydroxybenzaldehyde (6.0 g, 43.44 mmol), and piperidine (1 mL) were dissolved in ethanol (75 mL), and the resulting solution was heated under reflux for 4 h. After cooling, the precipitate was collected by filtration. The crude product was recrystallized from ethanol to afford the compound 13 as white solid (7.12 g, yield 70%). ¹H NMR (400 MHz, DMSO-*d*₆) δ: 11.06 (s, 1H), 8.66 (s, 1H), 7.76 (d, *J* = 8.4 Hz, 1H), 6.85 (dd, *J* = 8.4, 2.4 Hz, 1H), 6.72 (d, *J* = 2.4 Hz, 1H), 4.28 (q, 2H), 1.31 (t, 3H); ¹³C NMR (100 MHz, DMSO-*d*₆) δ: 164.02, 162.91, 157.07, 156.35, 149.35, 132.05, 113.96, 112.09, 110.39, 101.76, 60.76, 14.09; mp: 170–171 °C. ESI-MS (*m/z*): [M – H]⁺ 233.1.

Synthesis of Compound 14 (Ethyl-7-(2,4-dinitrophenoxy)-2-oxo-2H-chromene-3-carboxylate, Scheme 2). Compound 13 (117 mg, 0.5 mmol), 2,4-dinitrofluorobenzene (186 mg, 1.0 mmol), and anhydrous potassium carbonate (414 mg, 3 mmol) were added to a three-necked flask under N₂ atmosphere, and then anhydrous DMF (5 mL) was injected into the reaction flask with a syringe. The mixture was stirred at 80 °C until the starting material disappeared. The solvent was removed under reduced pressure, and the resulting residue was purified by chromatography on silica gel to give compound 14 (120 mg, yield 60%). ¹H NMR (400 MHz, DMSO-*d*₆) δ: 8.95 (d, *J* = 2.8 Hz, 1H), 8.81 (s, 1H), 8.56 (dd, *J* = 9.2, 2.8 Hz, 1H), 8.06 (d, *J* = 8.8 Hz, 1H), 7.54 (d, *J* = 9.2 Hz, 1H), 7.36 (d, *J* = 2.0 Hz, 1H), 7.29 (dd, *J* = 8.0, 2.4 Hz, 1H), 4.33 (q, 2H), 1.33 (t, 3H); ¹³C NMR (100 MHz, DMSO-*d*₆) δ: 162.99, 159.69, 156.62, 156.15, 153.23, 148.79, 143.49, 140.96, 133.06, 130.41, 122.74, 122.57, 116.90, 116.50, 115.74, 107.11, 61.72, 14.55; mp: 184–185 °C; ESI-MS (*m/z*): [M + H]⁺ 401.0.

Synthesis of Compound 15 (4-Amino-7-nitrobenzofurazan, Scheme 3).²⁴ To a solution of 4-chloro-7-nitrobenzofurazan (204 mg, 1 mmol) in MeOH (20 mL) was added ammonium hydroxide (4 mL, 30% in water) at room temperature. The reaction was stirred at room temperature for 24 h under nitrogen atmosphere. The solvent was evaporated in vacuo, and then the crude product was purified by silica gel chromatography to afford the product as a dark-green solid (108 mg, yield 60%). ¹H NMR (400 MHz, DMSO-*d*₆) δ: 8.87 (s, 1H), 8.51 (d, *J* = 8.8 Hz, 1H), 6.41 (d, *J* = 8.8 Hz, 1H); ¹³C NMR (100 MHz, DMSO-*d*₆) δ: 147.78, 144.79, 144.58, 138.46, 103.13; mp: 236–237 °C. ESI-MS (*m/z*): [M + H]⁺ 181.1.

Synthesis of Compound 16 (2,4-Dinitro-N-(7-nitrobenzo[*c*]-[1,2,5]oxadiazol-4-yl)benzenesulfonamide, Scheme 3).²⁴ To a solution of 15 (17 mg, 0.094 mmol) in anhydrous THF (2 mL) was added NaH (3.4 mg, 0.141 mmol) at 0 °C. After stirring for 15 min, 2,4-dinitrobenzenesulfonyl chloride (38 mg, 0.141 mmol) in 1.0 mL of anhydrous THF was added dropwisely to the reaction mixture. The reaction was warmed up to room temperature and stirred for another 1 h. Then the reaction mixture was quenched with saturated NaHCO₃ solution and extracted with ethyl acetate. The combined organic layer were washed with brine, dried with magnesium sulfate and evaporated in vacuo. The crude product was purified by silica gel chromatography affording desired product as an orange solid (24 mg, yield 62%). ¹H NMR (400 MHz, DMSO-*d*₆) δ: 8.76 (s, 1H), 8.51 (dd,

J = 8.4, 2.0 Hz, 1H), 8.41 (d, *J* = 8.8 Hz, 1H), 8.30 (d, *J* = 8.8 Hz, 1H), 6.69 (d, *J* = 8.8 Hz, 1H); ¹³C NMR (100 MHz, DMSO-*d*₆) δ: 150.89, 141.95, 136.01, 131.47, 126.01, 119.26, 107.70; mp: 172–173 °C; ESI-MS (*m/z*): [M + H]⁺ 409.1.

Synthesis of Compound 18 (7-Diethylamino-3-aminocoumarin, Scheme 3).⁴⁶ SnCl₂·2H₂O (19.4 g, 85.81 mmol) and 60 mL of 37% HCl were added to a 100 mL flask. Next, compound 17 (3.0 g, 11.45 mmol), which was prepared according to the literature⁴⁷ from 4-(diethylamino)salicylaldehyde, was added portion-wisely, and the resultant solution was further stirred at room temperature for 6 h. Then, a solution of 5 M NaOH was employed to neutralize the excessive acid, followed by extraction with ethyl acetate. The organic layer was dried with anhydrous Na₂SO₄ and evaporated to dryness. The crude product was purified by silica gel chromatography to afford desired product (1.27 g, yield 48%). ¹H NMR (400 MHz, DMSO-*d*₆) δ: 7.19 (d, *J* = 8.8 Hz, 1H), 6.68 (s, 1H), 6.61 (dd, *J* = 8.8, 2.4 Hz, 1H), 6.48 (d, *J* = 2.4 Hz, 1H), 4.99 (s, 2H), 3.36 (m, 4H), 1.09 (t, 6H); ¹³C NMR (100 MHz, DMSO-*d*₆) δ: 159.68, 150.84, 146.77, 129.14, 126.08, 111.55, 110.26, 109.66, 97.68, 44.19, 12.71; mp: 85–87 °C. ESI-MS (*m/z*): [M + H]⁺ 233.4.

Synthesis of Compound 19 (N-(7-(Diethylamino)-2-oxo-2H-chromen-3-yl)-2,4-dinitrobenzenesulfonamide, Scheme 3).⁴⁷ 2,4-Dinitrobenzenesulfonyl chloride (319 mg, 1.2 mmol) in 6 mL of CH₂Cl₂ was slowly added to the solution of 18 (232 mg, 1 mmol) and Et₃N (101 mg, 1 mmol) in 10 mL of CH₂Cl₂. The mixture was stirred overnight at room temperature. After the reaction was completed, the mixture was extracted with CH₂Cl₂ and dried over anhydrous Na₂SO₄. After removing the solvent under reduced pressure, the residue was purified by flash column chromatography to give the title compound as a red solid (147 mg, yield 32%). ¹H NMR (400 MHz, DMSO-*d*₆) δ: 10.56 (s, 1H), 8.86 (d, *J* = 2.0 Hz, 1H), 8.64 (dd, *J* = 8.8, 2.0 Hz, 1H), 8.32 (d, *J* = 8.4 Hz, 1H), 7.82 (s, 1H), 7.51 (d, *J* = 9.2 Hz, 1H), 6.75 (dd, *J* = 8.8, 2.0 Hz, 1H), 6.50 (d, *J* = 2.0 Hz, 1H), 3.45 (q, 4H), 1.27 (t, 6H); ¹³C NMR (100 MHz, DMSO-*d*₆) δ: 159.70, 155.53, 151.15, 150.21, 147.83, 140.93, 138.30, 132.53, 130.25, 127.36, 120.12, 114.43, 109.86, 107.56, 96.74, 44.51, 12.69; mp: 172–174 °C; ESI-MS (*m/z*): [M + H]⁺ 463.1; HRMS (*m/z*) [M + H]⁺ calcd for 463.0918, found 463.0907.

Synthesis of Compound 20 (7-Diethylamino-3-(4-nitrophenyl)-coumarin, Scheme 3).²³ 2,4-Dihydroxybenzaldehyde (345.3 mg, 2.5 mmol) and 4-nitrobenzyl cyanide (413 mg, 2.55 mmol) were dissolved in 5 mL ethanol, and five drops of piperidine were then added. The mixture was stirred at room temperature overnight. After filtration, the yellow solid was treated with 10% hydrochloric acid. The suspended solution was stirred at 130 °C overnight, and the resulting yellow residue was collected by filtration, washed with water, dried under reduced vacuum, and then purified by silica gel chromatography to afford the compound (420 mg, yield 50%). ¹H NMR (400 MHz, CDCl₃) δ: 8.26 (dd, *J* = 7.2, 2.0 Hz, 2H), 7.92 (dd, *J* = 7.2, 2.0 Hz, 2H), 7.82 (s, 1H), 8.26 (d, *J* = 9.2 Hz, 1H), 6.64 (dd, *J* = 8.8, 2.4 Hz, 1H), 6.54 (d, *J* = 2.0 Hz, 1H), 3.48 (q, 4H), 1.26 (t, 6H); EI-MS (*m/z*) (%): 338 (M⁺, 4), 193 (28), 44 (100).

Synthesis of Compound 21 (7-Diethylamino-3-(4-aminophenyl)-coumarin, Scheme 3). SnCl₂·2H₂O (19.4 g, 85.81 mmol) and 60 mL of 37% HCl were added to a 100 mL round-bottomed flask. Next, compound 20 (3.9 g, 11.45 mmol) was added portion-wisely, and the resultant solution was refluxed for 6 h. Then, a solution of 5 M NaOH was employed to neutralize the excessive acid, followed by extraction with ethyl acetate. The organic layer was dried with anhydrous Na₂SO₄ and evaporated to dryness. The crude product was purified by silica gel chromatography to afford desired product (1.27 g, yield 48%). ¹H NMR (400 MHz, DMSO-*d*₆) δ: 7.61 (s, 1H), 7.54 (m, 2H), 7.29 (t, 1H), 6.74 (m, 2H), 6.59 (dd, *J* = 8.8, 2.4 Hz, 1H), 6.53 (d, *J* = 2.4 Hz, 1H), 3.75 (s, 2H), 3.44 (q, 4H), 1.23 (t, 6H); ¹³C NMR (100 MHz, DMSO-*d*₆) δ: 161.95, 155.80, 150.04, 146.18, 138.53, 129.29, 128.50, 126.02, 121.14, 114.82, 109.38, 108.81, 97.22, 44.80, 12.48; mp: 178–180 °C. ESI-MS (*m/z*): [M + H]⁺ 309.0.

Synthesis of Compound 22 (N-(4-(7-Diethylamino-2-oxo-2H-chromen-3-yl)phenyl)-2,4-dinitrobenzenesulfonamide, Scheme 3). 2,4-Dinitrobenzenesulfonyl chloride (319 mg, 1.2 mmol) in 6 mL of

CH_2Cl_2 was slowly added to the solution of **21** (308 mg, 1 mmol) and Et_3N (101 mg, 1 mmol) in 20 mL of CH_2Cl_2 . The mixture was stirred overnight at room temperature. After the reaction was completed, the mixture was extracted with CH_2Cl_2 and dried with anhydrous Na_2SO_4 . After removing the solvent under reduced pressure, the residue was purified by flash column chromatography to give the title compound as a red solid (215 mg, yield 40%). ^1H NMR (400 MHz, $\text{DMSO}-d_6$) δ : 11.17 (s, 1H), 8.89 (d, $J = 2.4$ Hz, 1H), 8.63 (dd, $J = 8.8, 2.4$ Hz, 1H), 8.27 (d, $J = 8.8$ Hz, 1H), 8.02 (s, 1H), 7.66 (d, $J = 8.4$ Hz, 2H), 7.48 (d, $J = 8.8$ Hz, 1H), 7.19 (d, $J = 8.8$ Hz, 2H), 6.74 (dd, $J = 9.2, 2.4$ Hz, 1H), 6.54 (d, $J = 2.4$ Hz, 1H), 3.46 (q, 4H), 1.14 (s, 6H); ^{13}C NMR (100 MHz, $\text{DMSO}-d_6$) δ : 160.71, 156.09, 150.83, 150.42, 148.23, 141.23, 136.71, 135.47, 132.84, 131.94, 129.96, 129.30, 127.62, 120.83, 120.74, 118.10, 109.53, 108.71, 96.45, 44.43, 12.66; mp: 238–240 °C; ESI-MS (m/z): $[\text{M} - \text{H}]^+$ 537.14.

UV-vis and Fluorescence Spectroscopy. UV-vis spectra were acquired from UV-vis spectrometer evolution 200 (Thermo Scientific). Fluorescence spectroscopic studies were performed with a LUMINA fluorescence spectrophotometer (Thermo Scientific). The slit width was 2.5 nm for both excitation and emission. For absorption or fluorescence measurements, compounds were dissolved in DMSO or double distilled water to obtain stock solutions. These stock solutions were diluted with PBS to the desired concentration.

Screening of the Probes. DTT (10 mM, 10 μL), $(\text{Sec})_2$ (10 mM, 10 μL), probe (1 mM, 20 μL), and PBS were mixed to a final volume of 2000 μL . After incubating for 5 min at room temperature, the fluorescence intensity was measured. The $(\text{Sec})_2$ was omitted for determining the response of the probe to DTT.

Response of Sel-Green to Sec. The time-dependent absorbance spectra and fluorescence spectra ($\lambda_{\text{ex}} = 370$ nm) were acquired with the following procedures: Sel-green (10 μM) was incubated with DTT (50 μM) and $(\text{Sec})_2$ (50 μM) at room temperature in PBS, pH 7.4. The spectra were scanned every 1 min for 5 min. To acquire the emission spectra of Sel-green toward different concentrations of Sec, Sel-green (10 μM) was incubated with increasing concentrations of DTT and $(\text{Sec})_2$ at room temperature in PBS, pH 7.4. The emission spectra ($\lambda_{\text{ex}} = 370$ nm) were recorded after 2 min. The selectivity of Sel-green toward different analytes was studied as the following procedures. The fold of fluorescence increase at 502 nm ($\lambda_{\text{ex}} = 370$ nm) was determined after mixing Sel-green with various analytes for 2 min in PBS buffer, pH 7.4. Sec and BzSeH were generated from 50 μM $(\text{Sec})_2$ and 50 μM DBDS in the presence of 50 μM DTT, respectively, while the concentration of other analytes was 1 mM.

Kinetic Response of Sel-Green to Sec and Cys. Sel-green (10 μM) was incubated with DTT (50 μM) and $(\text{Sec})_2$ (50 μM) or different concentrations of Cys at room temperature in PBS, pH 7.4. The emission intensity at 502 nm ($\lambda_{\text{ex}} = 370$ nm) was measured every 30 s for 10 min. The fold of fluorescence increase (F/F_0) was normalized to the base fluorescence intensity of Sel-green.

pH-Dependent Fluorescence Response of Sel-Green to Sec and Cys. The fold of fluorescence increase at 502 nm ($\lambda_{\text{ex}} = 370$ nm) was determined after mixing Sel-green (10 μM) with DTT (50 μM) and $(\text{Sec})_2$ (50 μM) or Cys (1 mM) at room temperature for 2 min in different 0.1 M phosphate buffers (pH 5–9).

HPLC Analyses of the Reaction Between Sel-Green and Sec. Sel-green (48 mg, 0.1 mmol) was incubated with $(\text{Sec})_2$ (100 mg, 0.28 mmol) and DTT (42 mg, 0.28 mmol) in a DMSO-PBS mixed solvent (1:1, v/v) at room temperature for 1 h. The reaction mixture was dried under reduced pressure, and the residue was extracted with DCM. The combined solvent was removed under vacuum, and the residue was reconstituted in methanol. All samples were passed through a 0.22 μm filter, and 10 μL of sample was loaded onto the Waters symmetry C18, reversed-phase column (3.5 μm , 4.6 \times 75 mm) on a Waters 1525 binary HPLC system. The mixture of methanol and water (7:3, v/v) was used as eluent at the flow rate of 1.0 mL min^{-1} . The detection wavelength for Sel-green was set at 392 nm and for the fluorophore **18** was set at 337 nm.

Response of Sel-Green to TrxR and Other Proteins. The detection of Sec was performed at room temperature in PBS, pH 7.4. Sel-green (5 μL , 500 μM) was added to PBS buffer, followed by the addition of a

calculated amount of $(\text{Sec})_2$ and then 5 μL of DTT (1 mM) was added in a final volume of 50 μL . The fluorescence intensity was read after a 2 min incubation at room temperature. The calibration curve was constructed by plotting the folds of fluorescence change ($\lambda_{\text{ex}} = 370$ nm, $\lambda_{\text{em}} = 502$ nm) versus the concentrations of Sec. For the detection of the response of Sel-green to different proteins, all proteins were first adjusted to the concentration of 36 μM in PBS. DTT (1 mM, 5 μL) were incubated with a blank (30 μL TE buffer) or different proteins (30 μL) together with 10 μL PBS for 5 min at room temperature, and the probe (5 μL , 500 μM) was added to a final volume of 50 μL , and further incubating for 2 min. The fold of fluorescence change was measured. The protein concentrations of TrxR and U498C TrxR were calculated by measuring the absorbance of flavin at 460 nm ($\epsilon = 11.3 \text{ mM}^{-1} \text{ cm}^{-1}$),¹⁰ while others were calculated based on their stocks from vendors.

Imaging Sec in live HepG2 Cells. HepG2 cells were cultured in DMEM supplemented with 10% FBS, 2 mM glutamine, and 100 units/mL penicillin/streptomycin and maintained in an atmosphere of 5% CO_2 at 37 °C. The cells were seeded in 12-well plates at 2×10^4 cells per well in 1 mL growth medium and incubated at 37 °C for 24 h, and then the cells were exposed to $(\text{Sec})_2$ (5 μM) for 1 or 12 h. After washing with PBS three times to remove the remaining $(\text{Sec})_2$, the cells were further incubated with Sel-green (20 μM) for 30 min at 37 °C. After washing the cells with PBS three times, the fluorescence images were acquired with Fluid cell imaging station (life technology). To induce the endogenous Sec, the HepG2 cells were exposed to sodium selenite (5 μM) for 1h or 12 h, and then the cells were further incubated with the probe (20 μM) for 30 min at 37 °C. After washing the cells with PBS three times, the fluorescence images were acquired with Fluid cell imaging station.

Fluorescence Imaging of Selenol Species from Selenocompounds in Cells. The HepG2 and HeLa cells were seeded in 24-well plates at 1×10^4 cells per well in 0.5 mL growth medium and incubated at 37 °C for 24 h, and then the cells were exposed to different selenocompounds (5 μM) for 1, 6, and 12 h. After washing with PBS three times to remove the remaining selenocompounds in medium, the cells were further incubated with the probe Sel-green (20 μM) for 30 min at 37 °C. After washing the cells with PBS three times, the bright-field and fluorescence images were acquired with Fluid cell imaging station (Life Technology).

Cytotoxicity Assay. The cytotoxicity of different selenocompounds was determined by the MTT assay. Cells (5×10^3) were incubated with varying concentrations of the compounds in triplicate in a 96-well plate at 37 °C in a final volume of 100 μL . At the end of the treatment (20 h), 10 μL of MTT (5 mg/mL) was added to each well and incubated for an additional 4 h at 37 °C. An extraction buffer (100 μL , 10% SDS, 5% isobutanol, 0.1% HCl) was added, and the cells were incubated overnight at 37 °C. The absorbance was measured at 570 nm on Multiskan GO (Thermo Scientific). The cell viability was expressed as the percentage of the control (cells without drug treatment).

■ ASSOCIATED CONTENT

📄 Supporting Information

The original spectra (^1H NMR, ^{13}C NMR, and MS) of the final 18 compounds. This material is available free of charge via the Internet at <http://pubs.acs.org>.

■ AUTHOR INFORMATION

Corresponding Author

fangjg@lzu.edu.cn

Notes

The authors declare no competing financial interest.

■ ACKNOWLEDGMENTS

The financial supports from the Lanzhou University (the Fundamental Research Funds for the Central Universities,

lzujbky-2014-56), National Natural Science Foundation of China for Fostering Talents in Basic Research (J1103307), the 111 project, and Natural Science Foundation of Gansu Province (145RJZA225) are greatly acknowledged. The authors also express appreciation to Prof. Arne Holmgren (Karolinska Institute) for the recombinant rat TrxR.

REFERENCES

- (1) Schwarz, K.; Foltz, C. M. *J. Am. Chem. Soc.* **1957**, *79*, 3292.
- (2) Weekley, C. M.; Harris, H. H. *Chem. Soc. Rev.* **2013**, *42*, 8870.
- (3) Rayman, M. P. *Lancet* **2012**, *379*, 1256.
- (4) Ganther, H. E. *Carcinogenesis* **1999**, *20*, 1657.
- (5) Hatfield, D. L.; Tsuji, P. A.; Carlson, B. A.; Gladyshev, V. N. *Trends Biochem. Sci.* **2014**, *39*, 112.
- (6) Lu, J.; Holmgren, A. *J. Biol. Chem.* **2009**, *284*, 723.
- (7) Johansson, L.; Gafvelin, G.; Arner, E. S. *Biochim. Biophys. Acta* **2005**, *1726*, 1.
- (8) Stadtman, T. C. *Annu. Rev. Biochem.* **1996**, *65*, 83.
- (9) Huber, R. E.; Criddle, R. S. *Arch. Biochem. Biophys.* **1967**, *122*, 164.
- (10) Zhong, L.; Holmgren, A. *J. Biol. Chem.* **2000**, *275*, 18121.
- (11) Rocher, C.; Lalanne, J. L.; Chaudiere, J. *Eur. J. Biochem.* **1992**, *205*, 955.
- (12) Maeda, H.; Katayama, K.; Matsuno, H.; Uno, T. *Angew. Chem., Int. Ed. Engl.* **2006**, *45*, 1810.
- (13) Fang, J.; Holmgren, A. *J. Am. Chem. Soc.* **2006**, *128*, 1879.
- (14) Fang, J.; Lu, J.; Holmgren, A. *J. Biol. Chem.* **2005**, *280*, 25284.
- (15) Shannon, D. A.; Banerjee, R.; Webster, E. R.; Bak, D. W.; Wang, C.; Weerapana, E. *J. Am. Chem. Soc.* **2014**, *136*, 3330.
- (16) Niphakis, M. J.; Cravatt, B. F. *Annu. Rev. Biochem.* **2014**, *83*, 341.
- (17) Lanning, B. R.; Whitby, L. R.; Dix, M. M.; Douhan, J.; Gilbert, A. M.; Hett, E. C.; Johnson, T. O.; Joslyn, C.; Kath, J. C.; Niessen, S.; Roberts, L. R.; Schnute, M. E.; Wang, C.; Hulse, J. J.; Wei, B.; Whiteley, L. O.; Hayward, M. M.; Cravatt, B. F. *Nat. Chem. Biol.* **2014**, *10*, 760.
- (18) Weerapana, E.; Wang, C.; Simon, G. M.; Richter, F.; Khare, S.; Dillon, M. B.; Bachovchin, D. A.; Mowen, K.; Baker, D.; Cravatt, B. F. *Nature* **2010**, *468*, 790.
- (19) Macpherson, L. J.; Dubin, A. E.; Evans, M. J.; Marr, F.; Schultz, P. G.; Cravatt, B. F.; Patapoutian, A. *Nature* **2007**, *445*, 541.
- (20) Yin, C.; Huo, F.; Zhang, J.; Martinez-Manez, R.; Yang, Y.; Lv, H.; Li, S. *Chem. Soc. Rev.* **2013**, *42*, 6032.
- (21) Jung, H. S.; Chen, X.; Kim, J. S.; Yoon, J. *Chem. Soc. Rev.* **2013**, *42*, 6019.
- (22) Chen, X.; Zhou, Y.; Peng, X.; Yoon, J. *Chem. Soc. Rev.* **2010**, *39*, 2120.
- (23) Lin, W.; Long, L.; Tan, W. *Chem. Commun. (Cambridge)* **2010**, *46*, 1503.
- (24) Jiang, W.; Fu, Q.; Fan, H.; Ho, J.; Wang, W. *Angew. Chem., Int. Ed. Engl.* **2007**, *46*, 8445.
- (25) Maeda, H.; Matsuno, H.; Ushida, M.; Katayama, K.; Saeki, K.; Itoh, N. *Angew. Chem., Int. Ed. Engl.* **2005**, *44*, 2922.
- (26) Zhang, L.; Duan, D.; Liu, Y.; Ge, C.; Cui, X.; Sun, J.; Fang, J. *J. Am. Chem. Soc.* **2014**, *136*, 226.
- (27) Yao, J.; Ge, C.; Duan, D.; Zhang, B.; Cui, X.; Peng, S.; Liu, Y.; Fang, J. *J. Agric. Food Chem.* **2014**, *62*, 5507.
- (28) Liu, Y.; Duan, D.; Yao, J.; Zhang, B.; Peng, S.; Ma, H.; Song, Y.; Fang, J. *J. Med. Chem.* **2014**, *57*, 5203.
- (29) Duan, D.; Zhang, B.; Yao, J.; Liu, Y.; Sun, J.; Ge, C.; Peng, S.; Fang, J. *Free Radicals Biol. Med.* **2014**, *69*, 15.
- (30) Duan, D.; Zhang, B.; Yao, J.; Liu, Y.; Fang, J. *Free Radicals Biol. Med.* **2014**, *70*, 182.
- (31) Cai, W.; Zhang, L.; Song, Y.; Wang, B.; Zhang, B.; Cui, X.; Hu, G.; Liu, Y.; Wu, J.; Fang, J. *Free Radicals Biol. Med.* **2012**, *52*, 257.
- (32) Cai, W.; Zhang, B.; Duan, D.; Wu, J.; Fang, J. *Toxicol. Appl. Pharmacol.* **2012**, *262*, 341.
- (33) Zhang, L. W.; Duan, D. Z.; Cui, X. M.; Sun, J. Y.; Fang, J. G. *Tetrahedron* **2013**, *69*, 15.
- (34) Burnell, J. N.; Karle, J. A.; Shrift, A. *J. Inorg. Biochem.* **1980**, *12*, 343.
- (35) Zhong, L.; Arner, E. S.; Holmgren, A. *Proc. Natl. Acad. Sci. U. S. A.* **2000**, *97*, 5854.
- (36) Gladyshev, V. N.; Jeang, K. T.; Stadtman, T. C. *Proc. Natl. Acad. Sci. U. S. A.* **1996**, *93*, 6146.
- (37) Sun, R. W. Y.; Lok, C. N.; Fong, T. T. H.; Li, C. K. L.; Yang, Z. F.; Zou, T. T.; Siu, A. F. M.; Che, C. M. *Chem. Sci.* **2013**, *4*, 1979.
- (38) Zou, T.; Lum, C. T.; Lok, C. N.; To, W. P.; Low, K. H.; Che, C. M. *Angew. Chem., Int. Ed. Engl.* **2014**, *53*, 5810.
- (39) Rengby, O.; Cheng, Q.; Vahter, M.; Jornvall, H.; Arner, E. S. *Free Radic Biol. Med.* **2009**, *46*, 893.
- (40) Arner, E. S.; Sarioglu, H.; Lottspeich, F.; Holmgren, A.; Bock, A. *J. Mol. Biol.* **1999**, *292*, 1003.
- (41) Netto, L. E.; de Oliveira, M. A.; Monteiro, G.; Demasi, A. P.; Cussiol, J. R.; Discola, K. F.; Demasi, M.; Silva, G. M.; Alves, S. V.; Faria, V. G.; Horta, B. B. *Comp. Biochem. Physiol., Part C: Toxicol. Pharmacol.* **2007**, *146*, 180.
- (42) Shipton, M.; Kierstan, M. P.; Malthouse, J. P.; Stuchbury, T.; Brocklehurst, K. *FEBS Lett.* **1975**, *50*, 365.
- (43) Kryukov, G. V.; Castellano, S.; Novoselov, S. V.; Lobanov, A. V.; Zehtab, O.; Guigo, R.; Gladyshev, V. N. *Science* **2003**, *300*, 1439.
- (44) Spallholz, J. E. *Free Radicals Biol. Med.* **1994**, *17*, 45.
- (45) Rotruck, J. T.; Pope, A. L.; Ganther, H. E.; Swanson, A. B.; Hafeman, D. G.; Hoekstra, W. G. *Science* **1973**, *179*, 588.
- (46) Yu, D.; Huang, F.; Ding, S.; Feng, G. *Anal. Chem.* **2014**, *86*, 8835.
- (47) Li, J.; Zhang, C. F.; Yang, S. H.; Yang, W. C.; Yang, G. F. *Anal. Chem.* **2014**, *86*, 3037.
- (48) Wang, Z.; Han, D. M.; Jia, W. P.; Zhou, Q. Z.; Deng, W. P. *Anal. Chem.* **2012**, *84*, 4915.
- (49) Jiang, W.; Cao, Y.; Liu, Y.; Wang, W. *Chem. Commun. (Cambridge)* **2010**, *46*, 1944.
- (50) Narayanaperumal, S.; Alberto, E. E.; Gul, K.; Rodrigues, O. E.; Braga, A. L. *J. Org. Chem.* **2010**, *75*, 3886.
- (51) Nascimento, V.; Alberto, E. E.; Tondo, D. W.; Dambrowski, D.; Detty, M. R.; Nome, F.; Braga, A. L. *J. Am. Chem. Soc.* **2012**, *134*, 138.
- (52) Braga, A. L.; Wessjohann, L. A.; Taube, P. S.; Galetto, F. Z.; de Andrade, F. M. *Synthesis* **2010**, 3131.
- (53) Ma, S. F.; Fang, D. C.; Ning, B. M.; Li, M. F.; He, L.; Gong, B. *Chem. Commun. (Cambridge)* **2014**, *50*, 6475.
- (54) Song, L.; Yang, Y.; Zhang, Q.; Tian, H.; Zhu, W. *J. Phys. Chem. B* **2011**, *115*, 14648.
- (55) Liu, T. Y.; Zhang, X. F.; Qiao, Q. L.; Zou, C. Y.; Feng, L.; Cui, J. N.; Xu, Z. C. *Dyes Pigments* **2013**, *99*, 537.
- (56) Elzahabi, H. S. A. *Eur. J. Med. Chem.* **2011**, *46*, 4025.
- (57) Long, L.; Zhou, L.; Wang, L.; Meng, S.; Gong, A.; Du, F.; Zhang, C. *Org. Biomol. Chem.* **2013**, *11*, 8214.